of cases in the GWAS panel and estimated the accuracy between imputed and real genotypes by the square of the Pearson product-moment correlation coefficient ($R^2$).[30] We excluded a total of 10 SNPs from the replication analysis: 4 SNPs (rs141300960, rs70964082, rs36174706, and rs145599534) were excluded because of the difficulty of assay design, and 6 SNPs (rs79409596, rs239934, rs10252980, rs12688018, rs61054368, rs10871762) were excluded because they did not meet the accuracy threshold ($r^2 > 0.9$). For replication analysis of the remaining 34 candidates, we performed genotyping of 1158 cases in the replication cohort and examined the association with 15,061 replication controls for which we had imputed genotype data. We calculated combined association statistics using a meta-analysis between the imputed GWAS data and mixed replication data (cases using real genotypes with imputed control data).

### *Imputation for High-Density Mapping*

Imputation of the GWAS genotype data was performed using MACH v1.0[31] for 2 candidate loci including SNPs within an upstream or downstream 0.5-Mb margin. As reference haplotypes, we used genotype data for 286 East-Asian samples (CHB, 97; CHS, 100; JPT, 89) from 1094 individuals from the 1000 Genomes project released in June 2011.[29] In the process of imputation, 50 Markov chain iterations were implemented. To perform high-density mapping, we selected imputed SNPs with $P$ values of less than $1 \times 10^{-4}$ and tag SNPs based on HapMap Japanese data using Haploview software (available at: http://www.broadinstitute.org/scientific-community/science/programs/medical-and-population-genetics/haploview/downloads) ($r^2 > 0.9$; MAF $> 0.05$).[32] Genotyping of these SNPs was performed by a multiplex PCR-based Invader assay, and the same criteria for the replication study was applied (SNPs with HWE of $P \geq 0.001$ and samples with a call rate $\geq 0.98$). The concordance rate between imputed and assayed genotypes was 99.74% for 4p14 and 99.77% for 13q14.

### *Pathway, Protein–Protein Interaction, and Text Mining Analyses*

To define pathways and networks involved in CD pathogenesis, we selected 22 SNPs: 12 SNPs that showed nominal association in our replication cohort ($P < .05$) and 10 SNPs that showed association in our previous study.[33] First, we used the Gene Relationships Across Implicated Loci (GRAIL) method of literature-based pathway analysis to explore the connections between genes near our candidates.[34] GRAIL was applied to the 22 selected SNPs by using PubMed abstracts published before December 2006 (avoiding potential bias from the investigation of candidate genes stimulated by GWAS), the JPT+CHB Human HapMap, and the hg18 assembly of the human genome. Subsequently, we tested the hypothesis that a protein–protein interaction network built from these loci was enriched significantly for physical interactions by using DAPPLE.[35] We considered 2 categories of direct or indirect interactions and assessed the significance of the enrichment of physical interactions by permutation.

### *Statistical Analysis*

Association analysis was performed by the Cochran-Armitage trend test. Departure from HWE was evaluated using the chi-square test. We decided to use the significance threshold of $P = 5.0 \times 10^{-8}$ for the GWAS and $P = 7.94 \times 10^{-4}$ (calculated as $\alpha = .05$ for 63 tests after the Bonferroni correction) for the replication study. Combined analysis of the GWAS and the replication study was conducted by using the inverse variance–weighted method.[36] Heterogeneity among the studies was determined by using the Breslow–Day test. To estimate population structure, we performed PCA by using EIGENSTRAT version 3.0.[37] To draw the linkage disequilibrium (LD) map, we used Haploview software,[32] and LD was defined according to the published criteria.[38] For the association analysis for imputed genotypes, we used the R Bioconductor package, snpStats (available: http://www.bioconductor.org/packages/2.8/bioc/html/snpStats.html). We estimated the accuracy at each SNP with the square of the Pearson correlation coefficient between imputed and real genotypes ($r^2$). For general statistical analysis, we used R statistical environment version 2.12.1 (available: http://www.r-project.org/) or PLINK version 1.07.[39] Haplotype frequencies were estimated by using the expectation maximization (E-M) algorithm as implemented in the SNPHAP program (available: http://www.rfcgr.mrc.ac.uk/Menu/Help/snphap/). We estimated *cis*-expression quantitative trait loci (eQTL) signals based on the quantified data of immortalized B-lymphocytes from HapMap JPT data.[40] The data for individual genotypes for eQTL analysis was from the 1000 Genome project and was extracted with VCFtools software.[41]

## Results

### *A Genome-Wide Association Study and a Replication Study of CD*

We conducted a GWAS with 376 CD patients and 3397 control subjects in a Japanese population. All subjects were genotyped using the Illumina HumanHap550v3 BeadChip. After applying stringent quality control criteria (see Patients and Methods section), we performed an association analysis of 453,099 SNPs with MAF of 0.01 or greater in both the case and control groups. PCA showed no genetic heterogeneity among cases and controls (Supplementary Figure 1). A quantile–quantile plot (Supplementary Figure 2; including 2 reported loci: the major histocompatibility complex [MHC] region and *TNFSF15*[6,21]) shows the distribution of observed vs expected $P$ values, whereas the corresponding genomic inflation factor ($\lambda_{GC}$) of 1.037 suggests a low possibility of false-positive associations resulting from population stratification or cryptic relatedness. Our discovery panel is small compared with the current standards of GWAS; however, the combined study was estimated to have sufficient statistical power (~98.0% for the risk variant; odds ratio [OR], ~1.5; $\alpha = 5.0 \times 10^{-8}$; allele frequency, 0.1).

Our GWAS identified 19 SNPs that showed significant association with CD at the genome-wide level ($P < 5 \times 10^{-8}$). All of these SNPs are located in previously identified regions; 10 SNPs are in the MHC region, and the other 9 SNPs are in the 9q32 region (Figure 1). The top-associated SNP in the MHC region is rs7765379 ($P = 1.17 \times 10^{-15}$; OR, 1.95; 95% confidence interval [CI], 1.65–2.30), which is located between *HLA-DQB1* and *HLA-DQA2*. The most significant SNP in 9q32 is rs6478106 ($P = 1.64 \times 10^{-14}$; OR, 1.82; 95% CI, 1.55–2.12), which is located at the 3′ flanking region of the *TNFSF15* gene.

To identify new susceptibility loci for CD in the Japanese population, we performed a replication study with 1159 independent cases and 15,800 independent controls.

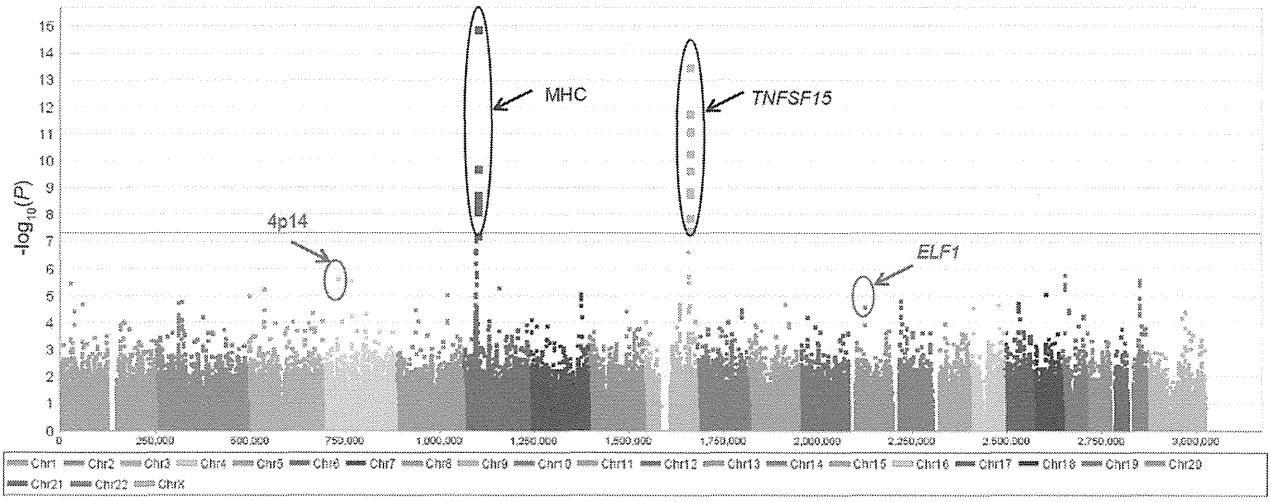


**Figure 1.** The result of the GWAS for CD. Manhattan plot for 453,099 SNPs from the GWAS for CD. SNPs are plotted according to chromosomal location, with the $-\log_{10}(P)$ calculated by the Cochran–Armitage test. The *red line* indicates the significance threshold for the GWAS ($P = 5.0 \times 10^{-8}$).

Among 98 SNPs with a $P$ value less than $1 \times 10^{-4}$, we identified 65 SNPs that represent independent loci after excluding 33 SNPs with strong LD ($r^2 > 0.9$). Among the 65 independent SNPs, 1 SNP (rs6739399) was excluded because genotype data from controls were not available in the replication set. Another SNP (rs6966614) was excluded because of the difficulty of assay design. After applying quality control criteria (see Patients and Methods section), we estimated the association of 63 SNPs successfully genotyped by the multiplex PCR-based Invader assay (Supplementary Table 1). Genotyping success rates in the replication study were 99.93% and 99.99% in cases and controls, respectively. We identified 3 SNPs whose association remained significant after the Bonferroni correction for multiple testing ($P < 7.94 \times 10^{-4}$): rs1487630 on 4p14 ($P = 3.52 \times 10^{-7}$), rs7329174 in the erythroid-like transcription factor family 1 (*ELF1*) on 13q14 ($P = 2.38 \times 10^{-5}$), and rs9891119 in *STAT3* on 17q21 ($P = 2.60 \times 10^{-11}$). The last SNP confirms the association of *STAT3* reported by an early meta-analysis of European subjects.[13] After combining the data from the GWAS and the replication study by using an inverse variance-weighted method, we identified 2 novel susceptibility loci for CD in the Japanese population (rs1487630 on 4p14: $P_{combined} = 1.29 \times 10^{-11}$; OR, 1.33; 95% CI, 1.22–1.44; rs7329174 on 13q14: $P_{combined} = 7.96 \times 10^{-9}$; OR, 1.27; 95% CI, 1.17–1.38) (Table 2). Because rs7329174 is an SNP associated with systemic lupus erythematosus in the Asian population,[42,43] the susceptibility region on 13q14 appears to be a common susceptibility locus for autoimmune diseases in the East-Asian population.

To search for additional candidate loci, we examined associations by using genome-wide imputed genotypes of GWAS samples. This analysis identified 44 candidate variants ($P < 1 \times 10^{-4}$). After applying quality control (see Patients and Methods section), we performed genotyping of 34 SNPs with sufficient accuracy by using 1158 cases in the replication cohort. Association analysis was performed by real genotype data in 1158 cases and imputed genotype data in 15,061 controls. As a result, rs11894081 on 2p25 showed a strong signal for CD in the Japanese population ($P = 3.58 \times 10^{-9}$) (Supplementary Table 2).

**Table 2.** Summary of Association Analysis With Novel Susceptibility Loci for Japanese CD Patients

| SNP region | Gene allele [1/2][a] | Stage | Case | | | Control | | | RAF | | $P^b$ | OR (95% CI)[c] | $P_{het}^d$ |
|---|---|---|---|---|---|---|---|---|---|---|---|---|---|
| | | | 11 | 12 | 22 | 11 | 12 | 22 | Case | Control | | | |
| rs1487630 | | GWAS | 35 | 156 | 181 | 170 | 1194 | 2023 | 0.30 | 0.23 | $2.24 \times 10^{-6}$ | 1.49 (1.26–1.76) | |
| 4p14 | [T/C] | Replication | 93 | 472 | 586 | 941 | 5652 | 9206 | 0.29 | 0.24 | $3.52 \times 10^{-7}$ | 1.28 (1.16–1.41) | |
| | | Combined | | | | | | | | | $1.29 \times 10^{-11}$ | 1.33 (1.22–1.44) | .48 |
| rs7329174 | *ELF1* | GWAS | 32 | 172 | 168 | 213 | 1241 | 1935 | 0.32 | 0.25 | $2.32 \times 10^{-5}$ | 1.42 (1.20–1.68) | |
| 13q14 | [G/A] | Replication | 106 | 467 | 578 | 1071 | 5908 | 8821 | 0.29 | 0.25 | $2.38 \times 10^{-5}$ | 1.22 (1.11–1.34) | |
| | | Combined | | | | | | | | | $7.96 \times 10^{-9}$ | 1.27 (1.17–1.38) | .48 |

RAF; risk allele frequency.

[a]Allele 1 is denoted as the risk allele.

[b]$P$ value was calculated by the Cochrane–Armitage trend test (1 degree of freedom), and combined results were estimated by inverse method-weighted ORs.

[c]Odds ratio of the risk allele is provided as a reference.

[d]Results of Breslow–Day test for the combined data.

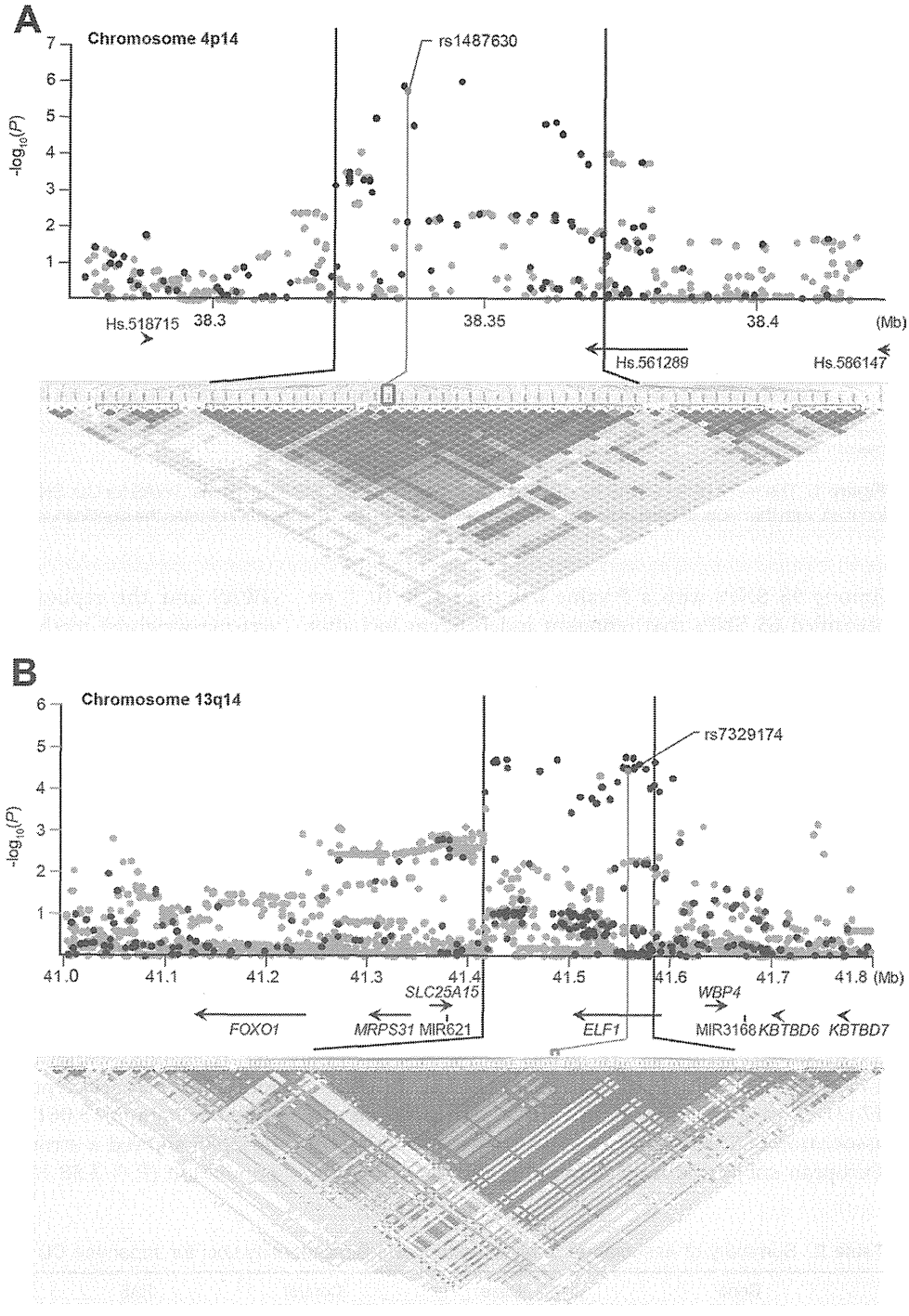


**Figure 2.** Case-control association results, LD map, and genomic structure of the regions on chromosomes (*A*) 4p14 and (*B*) 13q14. High-density mapping was performed in the regions (*A*) from 38.275 to 38.42 Mb on 4p14 and from (*B*) 41.35 to 41.8 Mb on 13q14. The *black dots* represent genotyped SNPs, and *gray dots* represent imputed SNPs. The *thick black line* represents the associated region defined by the LD block. The LD map based on D-prime values was drawn by using the genotype data of high-density mapping with markers of MAF greater than 0.2. The landmark SNPs on each region are indicated by a *red line*.

### *Fine Mapping of Two Identified Susceptibility Loci*

To further characterize these susceptibility regions, we performed high-density mapping around 2 markers identified in the GWAS. First, we imputed untyped markers in the GWAS data for the region of rs1487630 (±500 kb) using the 1000 Genomes project reference haplotypes (June 2011).[29] We constructed a regional plot for the 4p14 locus (Supplementary Figure 3*B*) and narrowed down the associated region to approximately 100 kb spanning from 38.3 to 38.4 Mb on chromosome 4. To clarify the susceptibility region of 4p14, we selected and genotyped a total of 76 SNPs by a multiplex PCR-based Invader assay: 9 SNPs that showed a $P$ value less than $1 \times 10^{-4}$ by imputation analysis and 67 tag SNPs selected from the HapMap phase II JPT data under the criteria of $r^2$ greater than 0.9 and MAF greater than 0.05 (Figure 2*A*; results of an association study with genotyped data are shown in Supplementary Table 3*A*).[25] The most highly associated SNPs were located within an LD block spanning approximately

50 kb from 38.32 to 38.37 Mb on chromosome 4. This high-density mapping found 2 additional SNPs that showed similar associations with rs1487630 ($P = 1.07 \times 10^{-6}$ for rs73243354 and $P = 1.22 \times 10^{-6}$ for rs73243351; Supplementary Table 3*A*). Because these 3 SNPs were in strong LD ($r^2 > 0.85$), haplotype analysis could not detect a stronger association than the single-marker association (Supplementary Figure 4*A*).

For the second susceptibility region on chromosome 13q14, we also performed imputation around the associated marker of rs7329174 (Supplementary Figure 3*B*). Our imputation analysis found that associated variants spanned a wide region from 41.4 to 41.8 Mb on 13q14. To narrow down the candidate region around rs7329174, we genotyped a total of 190 SNPs including 33 imputed SNPs and 157 tag-SNPs (Supplementary Table 3*B*). This high-density mapping identified an additional 15 SNPs that showed the same strength of association as rs7329174, and these SNPs were located within a 174-kb LD block (Figure 1*B*). We also performed haplotype analysis with 16 highly associated SNPs, but no haplotype showed a stronger association than was observed using single markers (Supplementary Figure 4*B*).

### *eQTL Analysis and Pathway Analysis*

To identify promising regional transcripts, we examined the effect of associated SNPs on the expression of 2 loci by using the available eQTL data.[40] On 4p14, none of these 3 SNPs affected the expression level of a likely candidate gene locus, the nearby *Toll-like receptor* (*TLR*) gene cluster (Supplementary Figure 5*A*). We also attempted to apply eQTL analysis of 16 associated SNPs to *ELF1*, *SLC25A15*, and *WBP4* around rs7329174 on 13q14. Although these SNPs did not affect the expression of *ELF1* or *WBP4*, we found that the associated SNPs upregulated the expression level of *SLC25A15* ($P = .00055$, $P_{FDR\ (False\ Discovery\ Rate)} = .0090$ between *SLC25A15* and rs7329474/rs57088152; Supplementary Figure 5*B*). These results suggest that *ELF1* or *SLC25A15* are candidate susceptibility genes for CD in this region. Further functional studies will be required to clarify the biological role to confer CD susceptibility.

We extended 2 pathway analyses by using GRAIL[34] and DAPPLE[35] to identify connections among our single-marker associations and link them with broader biological processes. As candidates for these analyses, we selected 22 SNPs: 12 variants that showed associations in this study and 10 SNPs that were replicated in our previous report.[33] To analyze the functional connections among them, we used the GRAIL method of literature-based pathway analysis to explore the connections between genes near our candidates. Six regions had significant GRAIL scores (Supplementary Table 4). This analysis indicated that there were strong connections between our 2 dominant signals at the MHC region and *TNFSF15*. The top associated region around *HLA-DQA1* was functionally related to multiple genes (Supplementary Figure 6). Subsequently, we constructed a network of proteins from these 22 loci by using DAPPLE.[35] However, neither the direct (between the associated transcripts themselves) nor the indirect (via common interactors that were not among the associated transcripts) connectivities were statistically significant ($P_{permuted}$ for direct-connectivity = .19; $P_{permuted}$ for indirect = .52; Supplementary Figure 7).

## Discussion

IBD, CD, and ulcerative colitis are multifactorial diseases characterized by remitting and relapsing inflammation in the gut.[1] Although genetic differences for CD susceptibility loci are known,[18-20,33] most CD susceptibility loci were derived from cohorts of European ancestry.[7,12-14] Recently, the International IBD Genetics Consortium identified an additional 71 associations using a meta-analysis of more than 75,000 cases and controls.[44] Combined with previous reports, a total of 163 IBD loci over genome-wide significance thresholds have been identified. However, there have been few GWAS data in East-Asian populations.[6,21] Here, to explore new susceptibility loci for CD in the East-Asian population, we performed a GWAS and a replication study with a total of 1523 Japanese CD cases and 19,189 controls. As a result, we identified 2 novel loci that confer CD susceptibility in the Japanese population. By using genome-wide imputation analysis, we identified one additional candidate locus for CD susceptibility. These 3 loci did not overlap with those found in the latest report from the International IBD Genetics Consortium.[44]

Around the susceptibility region of chromosome 4p14, there are no protein-coding genes or known micro RNAs from the database miRBase (http://www.mirbase.org/). According to the UniGene database (http://www.ncbi.nlm.nih.gov/unigene), 2 expression sequence tags, Hs.518715 and Hs.561289, are mapped around this region. However, the functions of these expression sequence tags are mostly unknown. A TLR gene cluster (*TLR10*, *TLR1*, and *TLR6*) is located approximately 500 kb from the susceptibility region on the centromeric side. TLRs are primary triggers of the innate immune system by recognizing various microorganisms through conserved pathogen-associated molecular patterns.[45] Therefore, we examined the effect of the top 3 associated SNPs on the expression of the *TLR* gene cluster by using the available eQTL data.[40] However, none of these 3 SNPs affect the expression level of these genes (Supplementary Figure 5*A*).

The associated region of 13q14 encompassed the *ELF1* gene. The encoded protein of *ELF1* is implicated in the transcriptional regulation of T-cell–specific genes such as CD4 and plays an important role in the ontogeny and function of invariant natural killer T cells.[46,47] It was reported that invariant natural killer T cells provide a natural barrier against the Th17 response in a mouse model of experimental autoimmune encephalomyelitis.[48] Therefore, the *ELF1* gene is a candidate for CD susceptibility in this region. Several other genes are located around this region; MIR2276 (microRNA) and *SLC25A15*

are located on the centromeric side, and *WBP4* is located on the telomeric side. The encoded protein of *SLC25A15* transports ornithine across the inner mitochondrial membrane from the cytosol to the mitochondrial matrix. Mutations in *SLC25A15* cause hyperornithinemia-hyperammonemia-homocitrullinuria syndrome.[49] The *WBP4* gene encodes FBP21, which plays a role in the cross-intron bridging of U1 and U2 snRNPs in spliceosomal complex A.[50] By our eQTL analysis, the susceptibility alleles on 13q14 will up-regulate the expression level of *SLC25A15* (Supplementary Figure 5*B*). Further functional studies are required to clarify the biological role of this region in conferring CD susceptibility.

By performing an association study using genome-wide imputation of the GWAS subjects' data, we identified rs11894081 as a suggestive locus for conferring CD susceptibility. The nearest gene to rs11894081 was *SOX11* (sex determining region Y-box 11). Although aberrant expression of SOX11 activates histone marks in some B-cell neoplasms,[51] the relationship between *SOX11* and CD is unknown. Moreover, this association was obtained from analysis of real genotype data for cases and imputed genotype data for controls. Further studies are needed to clarify the association.

In European ancestry CD, dominant signals were observed at *NOD2* and *IL23R*, with only modest signals observed within the MHC.[13,14] In contrast, the genetic architecture of Japanese CD was dominated by 2 signals at the MHC and *TNFSF15*. For systematic comparison, we extracted the GWAS data of SNPs with nominal association ($P < .01$) in the 71 regions defined by a previous report using subjects of European descent (Supplementary Table 5).[14] Although the allele frequencies of causal variants in *NOD2* were very low in the Japanese population,[18,33] different SNPs showed nominal association in Japanese CD patients. For the *IL23R* region, there was no associated SNP in Japanese CD patients. The strong signals around the MHC class II molecules may be caused by the ethnic differences in the MHC region, as described previously.[21] The *STAT3* gene has been identified as a common susceptibility gene, but the most associated SNP in Japanese CD patients differed from that found in European populations. Our data provide details of the difference in the genetic architecture of CD between Japanese and European CD patients.

In conclusion, we identified 2 new susceptibility loci for CD at 4p14 (spanning from 38.32 to 38.37 MB) and 13q14 (spanning from 41.416 to 41.59 MB) in the Japanese population. Further functional studies of these loci will provide a better understanding of the pathogenesis of CD.

## Supplementary Material

Note: To access the supplementary material accompanying this article, visit the online version of *Gastroenterology* at www.gastrojournal.org, and at http://dx.doi.org/10.1053/j.gastro.2012.12.021.

## References


1. Podolsky DK. Inflammatory bowel disease. N Engl J Med 2002; 347:417–429.
2. Asakura K, Nishiwaki Y, Inoue N, et al. Prevalence of ulcerative colitis and Crohn's disease in Japan. J Gastroenterol 2009;44: 659–665.
3. Goh K, Xiao S. Inflammatory bowel disease: a survey of the epidemiology in Asia. J Dig Dis 2009;10:1–6.
4. Cho JH. The genetics and immunopathogenesis of inflammatory bowel disease. Nat Rev Immunol 2008;8:458–466.
5. Budarf ML, Labbé C, David G, et al. GWA studies: rewriting the story of IBD. Trends Genet 2009;25:137–146.
6. Yamazaki K, McGovern D, Ragoussis J, et al. Single nucleotide polymorphisms in TNFSF15 confer susceptibility to Crohn's disease. Hum Mol Genet 2005;14:3499–3506.
7. Duerr RH, Taylor KD, Brant SR, et al. A genome-wide association study identifies IL23R as an inflammatory bowel disease gene. Science 2006;314:1461–1463.
8. Rioux JD, Xavier RJ, Taylor KD, et al. Genome-wide association study identifies new susceptibility loci for Crohn disease and implicates autophagy in disease pathogenesis. Nat Genet 2007; 39:596–604.
9. Hampe J, Franke A, Rosenstiel P, et al. A genome-wide association scan of nonsynonymous SNPs identifies a susceptibility variant for Crohn disease in ATG16L1. Nat Genet 2007;39:207–211.
10. Libioulle C, Louis E, Hansoul S, et al. Novel Crohn disease locus identified by genome-wide association maps to a gene desert on 5p13.1 and modulates expression of PTGER4. PLoS Genet 2007; 3:e58.
11. Parkes M, Barrett JC, Prescott NJ, et al. Sequence variants in the autophagy gene IRGM and multiple other replicating loci contribute to Crohn's disease susceptibility. Nat Genet 2007;39:830–832.
12. The Wellcome Trust Case Control Consortium. Genome-wide association study of 14,000 cases of seven common diseases and 3,000 shared controls. Nature 2007;447:661–678.
13. Barrett JC, Hansoul S, Nicolae DL, et al. Genome-wide association defines more than 30 distinct susceptibility loci for Crohn's disease. Nat Genet 2008;40:955–962.
14. Franke A, McGovern DPB, Barrett JC, et al. Genome-wide meta-analysis increases to 71 the number of confirmed Crohn's disease susceptibility loci. Nat Genet 2010;42:1118–1125.
15. Manolio TA, Collins FS, Cox NJ, et al. Finding the missing heritability of complex diseases. Nature 2009;461:747–753.
16. Hilmi I, Tan YM, Goh KL. Crohn's disease in adults: observations in a multiracial Asian population. World J Gastroenterol 2006;12: 1435–1438.
17. Wang YF, Zhang H, Ouyang Q. Clinical manifestations of inflammatory bowel disease: East and West differences. J Dig Dis 2007;8:121–127.
18. Yamazaki K, Takazoe M, Tanaka T, et al. Absence of mutation in the NOD2/CARD15 gene among 483 Japanese patients with Crohn's disease. J Hum Genet 2002;47:469–472.
19. Yamazaki K, Onouchi Y, Takazoe M, et al. Association analysis of genetic variants in IL23R, ATG16L1 and 5p13.1 loci with Crohn's disease in Japanese patients. J Hum Genet 2007;52:575–583.
20. Yamazaki K, Takahashi A, Takazoe M, et al. Positive association of genetic variants in the upstream region of NKX2-3 with Crohn's disease in Japanese patients. Gut 2009;58:228–232.
21. Okada Y, Yamazaki K, Umeno J, et al. HLA-Cw*1202-B*5201-DRB1*1502 haplotype increases risk for ulcerative colitis but reduces risk for Crohn's disease. Gastroenterology 2011;141: 864–871.e1–5.
22. Lennard-Jones JE. Classification of inflammatory bowel disease. Scand J Gastroenterol Suppl 1989;170:2–6; discussion, 16–9.
23. Asano K, Matsushita T, Umeno J, et al. A genome-wide association study identifies three new susceptibility loci for ulcerative colitis in the Japanese population. Nat Genet 2009;41:1325–1329.

24. Nakamura Y. The BioBank Japan Project. Clin Adv Hematol Oncol 2007;5:696–697.
25. The International Hapmap Consortium. A haplotype map of the human genome. Nature 2005;437:1299–1320.
26. Yamaguchi-Kabata Y, Nakazono K, Takahashi A, et al. Japanese population structure, based on SNP genotypes from 7003 individuals compared to other ethnic groups: effects on population-based association studies. Am J Hum Genet 2008;83:445–456.
27. Okada Y, Hirota T, Kamatani Y, et al. Identification of nine novel loci associated with white blood cell subtypes in a Japanese population. PLoS Genetics 2011;7:e1002067.
28. Howie BN, Donnelly P, Marchini J. A flexible and accurate genotype imputation method for the next generation of genome-wide association studies. PLoS Genet 2009;5:e1000529.
29. The 1000 Genomes Project Consortium. A map of human genome variation from population-scale sequencing. Nature 2010;467: 1061–1073.
30. Zheng J, Li Y, Abecasis GR, et al. A comparison of approaches to account for uncertainty in analysis of imputed genotypes. Genet Epidemiol 2011;35:102–110.
31. Li Y, Willer CJ, Ding J, et al. MaCH: using sequence and genotype data to estimate haplotypes and unobserved genotypes. Genet Epidemiol 2010;34:816–834.
32. Barrett J, Fry B, Maller J. Haploview: analysis and visualization of LD and haplotype maps. Bioinformatics 2005;21:263–265.
33. Hirano A, Yamazaki K, Umeno J, et al. Association study of 71 European Crohn's disease susceptibility loci in a Japanese population. Inflamm Bowel Dis. In press.
34. Raychaudhuri S, Plenge RM, Rossin EJ, et al. Identifying relationships among genomic disease regions: predicting genes at pathogenic SNP associations and rare deletions. PLoS Genet 2009;5: e1000534.
35. Rossin EJ, Lage K, Raychaudhuri S, et al. Proteins encoded in genomic regions associated with immune-mediated disease physically interact and suggest underlying biology. PLoS Genet 2011; 7:e1001273.
36. Bakker PIW de, Ferreira MAR, Jia X, et al. Practical aspects of imputation-driven meta-analysis of genome-wide association studies. Hum Mol Genet 2008;17:R122–R1228.
37. Price AL, Patterson NJ, Plenge RM, et al. Principal components analysis corrects for stratification in genome-wide association studies. Nat Genet 2006;38:904–909.
38. Gabriel SB, Schaffner SF, Nguyen H, et al. The structure of haplotype blocks in the human genome. Science 2002;296:2225–2229.
39. Purcell S, Neale B, Todd-Brown K, et al. PLINK: a tool set for whole-genome association and population-based linkage analyses. Am J Hum Genet 2007;81:559–575.
40. Stranger BE, Forrest MS, Dunning M, et al. Relative impact of nucleotide and copy number variation on gene expression phenotypes. Science 2007;315:848–853.
41. Danecek P, Auton A, Abecasis G, et al. The variant call format and VCFtools. Bioinformatics 2011;27:2156–2158.
42. Yang J, Yang W, Hirankarn N, et al. ELF1 is associated with systemic lupus erythematosus in Asian populations. Hum Mol Genet 2011;20:601–607.
43. Okada Y, Shimane K, Kochi Y, et al. A genome-wide association study identified AFF1 as a susceptibility locus for systemic lupus eyrthematosus in Japanese. PLoS Genet 2012;8:e1002455.
44. Jostins L, Ripke S, Weersma RK. Host-microbe interactions have shaped the genetic architecture of inflammatory bowel disease. Nature 2012;490:119–124.
45. Kawai T, Akira S. The role of pattern-recognition receptors in innate immunity: update on Toll-like receptors. Nat Immunol 2010;11:373–384.
46. Sarafova S, Siu G. A potential role for Elf-1 in CD4 promoter function. J Biol Chem 1999;274:16126–16134.
47. Choi H-J, Geng Y, Cho H, et al. Differential requirements for the Ets transcription factor Elf-1 in the development of NKT cells and NK cells. Blood 2011;117:1880–1887.
48. Mars LT, Araujo L, Kerschen P, et al. Invariant NKT cells inhibit development of the Th17 lineage. Proc Natl Acad Sci U S A 2009;106:6238–6243.
49. Camacho JA, Obie C, Biery B, et al. Hyperornithinaemia-hyperammonaemia-homocitrullinuria syndrome is caused by mutations in a gene encoding a mitochondrial ornithine transporter. Nat Genet 1999;22:151–158.
50. Bedford MT, Reed R, Leder P. WW domain-mediated interactions reveal a spliceosome-associated protein that binds a third class of proline-rich motif: the proline glycine and methionine-rich motif. Proc Natl Acad Sci U S A 1998;95:10602–10607.
51. Vegliante MC, Royo C, Palomero J, et al. Epigenetic activation of SOX11 in lymphoid neoplasms by histone modifications. PLoS One 2011;6:e21382.

Received April 16, 2012. Accepted December 17, 2012.

*Reprint requests*

Address requests for reprints to: Michiaki Kubo, MD, PhD, Laboratory for Genotyping Development, Center for Genomic Medicine, Riken Yokohama Institute, 1-7-22 Suehiro-Cho, Tsurumi-Ku, Yokohama, Kanagawa 230-0045, Japan. e-mail: mkubo@src.riken.jp; fax: (81) 45-503-9606.

*Acknowledgments*

The authors thank the members of the BioBank Japan project and the Rotary Club of Osaka-Midosuji District 2660 Rotary International in Japan; all patients with Crohn's disease and their families for their contribution to this project; and Ai Maejima, Mayumi Nakayama, Takako Tokugawa, Yuko Sumikawa, Kyota Ashikawa, Tomomi Aoi, and the other members of the Laboratory for Genotyping Development for their technical assistance.

*Conflicts of interest*

The authors disclose no conflicts.

*Funding*

Supported by a grant from the BioBank Japan Project and in part by a Grant-in-Aid for Young Scientists (A) (22689025) from the Ministry of Education, Culture, Sports, Science and Technology.

# Increased Th17-Inducing Activity of CD14$^+$ CD163$^{low}$ Myeloid Cells in Intestinal Lamina Propria of Patients With Crohn's Disease

TAKAYUKI OGINO,[1] JUNICHI NISHIMURA,[1] SOUMIK BARMAN,[2,3] HISAKO KAYAMA,[2,3] SATOSHI UEMATSU,[4] DAISUKE OKUZAKI,[5] HIDEKI OSAWA,[1] NAOTSUGU HARAGUCHI,[1] MAMORU UEMURA,[1] TAISHI HATA,[1] ICHIRO TAKEMASA,[1] TSUNEKAZU MIZUSHIMA,[1] HIROFUMI YAMAMOTO,[1] KIYOSHI TAKEDA,[2,3,6] YUICHIRO DOKI,[1] and MASAKI MORI[1]

*[1]Department of Gastroenterological Surgery, [2]Laboratory of Immune Regulation, Graduate School of Medicine, Osaka University, Osaka, Japan; [3]Laboratory of Mucosal Immunology, Immunology Frontier Research Center, Osaka University, Osaka, Japan; [4]Division of Innate Immune Regulation, International Research and Development Center for Mucosal Vaccines, Institute of Medical Science, Tokyo University, Tokyo, Japan; [5]DNA-Chip Developemental Center for Infectious Diseases, Research Institute for Microbial Diseases, Osaka University, Osaka, Japan; and [6]Core Research for Evolutional Science and Technology, Japan Science and Technology Agency, Saitama, Japan*

**BACKGROUND & AIMS:** Abnormal activity of innate immune cells and T-helper (Th) 17 cells has been implicated in the pathogenesis of autoimmune and inflammatory diseases, including Crohn's disease (CD). Intestinal innate immune (myeloid) cells have been found to induce development of Th17 cells in mice, but it is not clear if this occurs in humans or in patients with CD. We investigated whether human intestinal lamina propria cells (LPCs) induce development of Th17 cells and whether these have a role in the pathogenesis of CD. **METHODS:** Normal intestinal mucosa samples were collected from patients with colorectal cancer and noninflamed and inflamed regions of mucosa were collected from patients with CD. LPCs were isolated by enzymatic digestion and analyzed for expression of HLA-DR, lineage markers CD14 and CD163 using flow cytometry. **RESULTS:** Among HLA-DR$^{high}$ Lin$^-$ cells, we identified a subset of CD14$^+$ CD163$^{low}$ cells in intestinal LPCs; this subset expressed Toll-like receptor (*TLR*) *2*, *TLR4*, and *TLR5* mRNAs and produced interleukin (IL)-6, IL-1$\beta$, and tumor necrosis factor in response to lipopolysaccharide. In vitro co-culture with naïve T cells revealed that CD14$^+$ CD163$^{low}$ cells induced development of Th17 cells. CD14$^+$ CD163$^{low}$ cells from inflamed regions of mucosa of patients with CD expressed high levels of *IL-6*, *IL-23p19*, and tumor necrosis factor mRNAs, and strongly induced Th17 cells. CD14$^+$ CD163$^{low}$ cells from the noninflamed mucosa of patients with CD also had increased abilities to induce Th17 cells compared with those from normal intestinal mucosa. **CONCLUSIONS: CD14$^+$ CD163$^{low}$ cells in intestinal LPCs from normal intestinal mucosa induce differentiation of naive T cells into Th17 cells; this activity is increased in mucosal samples from patients with CD. These findings show how intestinal myeloid cell types could contribute to pathogenesis of CD and possibly other Th17-associated diseases.**

*Keywords:* Dendritic Cell; Macrophage; Helper T Cell; Inflammatory Bowel Disease.

Recent studies have suggested that innate immune cells, including macrophages and dendritic cells (DC) of the intestinal mucosa, play important roles in maintaining gut homeostasis by protecting the host from foreign pathogens and by negatively regulating excess immune responses to commensal bacteria and dietary antigens.[1,2] Inappropriate immune reactions to commensal bacteria can lead to development of inflammatory bowel diseases (IBD), such as Crohn's disease (CD) and ulcerative colitis.[3,4] The identification of interleukin (IL)-17–producing Th17 cells offers new insight into the induction and regulation of mucosal immunity, which is linked to IBD pathogenesis.[5–7] Additionally, genome-wide association studies have shown significant associations of CD with Th17-related inflammatory pathways and innate microorganism sensors.[8–13]

Several subsets of murine intestinal innate immune cells have been found to modulate intestinal homeostasis.[14] In the CD11c$^+$ cell subset, CD103$^+$ and CX3CR1$^+$ cells represent nonoverlapping populations with different precursors.[15–17] CD103$^+$ cells uptake luminal antigens in the lamina propria by a unique mechanism, move to the mesenteric lymph nodes (MLN), and activate T cells.[18,19] They can induce expression of gut homing receptors (CCR9 and $\alpha 4\beta 7$ integrin) on T cells, activate CD8$^+$ T cells, and induce differentiation of Foxp3-expressing regulatory T cells.[20–22] CX3CR1$^+$ cells can be divided into 2 subsets based on CX3CR1 expression level: CX3CR1$^{int}$ and CX3CR1$^{high}$ cells.[15,23] CX3CR1$^{int}$ cells are DCs that induce Th17 cells and migrate into the inflammatory regions,[23–28] and CX3CR1$^{high}$ cells possess anti-inflammatory properties and inhibit T-cell responses.[26,29,30] These findings strongly support the notion that intestinal innate immune cells regulate gut homeostasis.

Compared with murine intestinal innate immune cells, human intestinal cells remain less well characterized. It

*Abbreviations used in this paper:* CD, Crohn's disease; CDi, inflamed region of CD; CDn, noninflamed region of CD; DC, dendritic cell; IBD, inflammatory bowel disease; IFN, interferon; IL, interleukin; int, intermediate; LPC, lamina propria cell; MLN, mesenteric lymph node; mRNA, messenger RNA; NC, normal colon from colon cancer patients; slan, 6-sulfo LacNAc; TGF, transforming growth factor; Th, T-helper; TLR, Toll-like receptor; TNF, tumor necrosis factor.


0016-5085/$36.00
http://dx.doi.org/10.1053/j.gastro.2013.08.049

has been reported that resident intestinal macrophages fail to produce proinflammatory cytokines in response to Toll-like receptor (TLR) ligands, in spite of active phagocytic and bactericidal activities.[31,32] A unique subset of macrophages that express macrophage (CD14, CD33, CD68) and DC (CD205, CD209) markers reportedly contributes to IBD pathogenesis through induction of IL-23–dependent interferon (IFN) gamma responses by T cells, as well as potent antigen-presenting activity.[33,34] Similar to the mouse intestinal $CD103^+$ cells, $CD103^+$ DCs that can induce gut homing receptors have been identified in the human small intestine.[20] However, human intestinal lamina propria cells (LPCs) equivalent to mouse $CX3CR1^+$ cells have not yet been characterized. Most recently, human LPCs have been classified into subsets based on the expressions of CD14, HLA-DR, CD209, CD163, and CD11c.[28] However, functional characterization of these human LPC subsets remains elusive.

In the present study, we show that HLA-$DR^{high}$ $Lin^-$ cells in human intestinal lamina propria comprise 4 subsets that are distinguished by differential expression patterns of CD14, CD11c, and CD163. We further show that HLA-$DR^{high}$ $Lin^-$ $CD14^+$ $CD163^{low}$ cells induce Th17 cell differentiation. CD patients exhibited exceedingly enhanced Th17 immunity induced by HLA-$DR^{high}$ $Lin^-$ $CD14^+$ $CD163^{low}$ cells, even in noninflamed intestine.

## Methods

### *Tissue Samples*

Normal intestinal mucosa was obtained from microscopically and macroscopically intact areas in patients with colorectal cancer. Intestinal mucosa was also obtained from surgically resected specimens from patients with CD who were diagnosed based on established clinical, bacteriological, radiologic, and endoscopic criteria. Histopathological analysis showed moderate to severe inflammation in all samples from patients with CD. This study was approved by the Ethical Committee of Osaka University School of Medicine and informed consent for specimen use was obtained from all patients.

### *Isolation of LPCs*

To isolate LPCs, intestinal mucosa was washed in phosphate-buffered saline to remove feces. Then, intestinal mucosa was placed in RPMI 1640 containing 5 mM EDTA and incubated for 10 minutes in a 37°C shaking water bath. After washing in phosphate-buffered saline, the mucosa was cut into small pieces and incubated in RPMI 1640 containing 10% fetal bovine serum, 2 mg/mL collagenase D (Roche, Basel, Switzerland), 1 mg/mL dispase (Invitrogen, Carlsbad, CA), and 15 μg/mL DNase I (Roche) for 60 minutes in a 37°C shaking water bath. The digested tissues were then passed through a 40-μm cell strainer. The isolated cells were washed with RPMI 1640 containing 5 mM EDTA, resuspended in 5 mL 20% Percoll (GE Healthcare Japan, Tokyo, Japan), and then overlaid on 2.5 mL 40% Percoll in a 15-mL tube. Percoll gradient separation was performed by centrifugation at 500*g* for 30 min at 4°C. The LPCs were collected from the interface of the Percoll gradient, then washed twice with phosphate-buffered saline containing 2% fetal bovine serum.

### *Flow Cytometry*

The antibodies for flow cytometry are shown in the Supplementary Material. Flow cytometric analysis was performed using a FACSCantoII flow cytometer (BD Biosciences, San Jose, CA). LPCs were purified using a FACSAriaII system (BD Biosciences), and data were analyzed with FlowJo software (Tree Star, Ashland, OR).

### *Morphological Analysis*

Isolated LPC subsets were spread on glass slides and were air dried. The spread cells were fixed with methanol, stained by May-Grünwald-Giemsa method, and observed with a microscope (BZ-9000; KEYENCE, Itasca, IL).

### *Microarray Analysis*

Total RNA derived from LPCs was reverse transcribed by using an Ovation Pico WTA System V2 (NuGen, San Carlos, CA) and labeled with cyanine-3 using a Genomic DNA Enzymatic Labeling Kit (Agilent Technologies, Santa Clara, CA). The labeled complementary DNA was hybridized to SurePrint G3 Human Gene Expression v2 8x60K Microarray (G4845A) (Agilent Technologies). The data have been deposited in GEO as GSE49066. See the Supplemental Material for more details.

### *Quantitative Real-Time Reverse Transcription Polymerase Chain Reaction*

Total RNA was isolated using the RNeasy Mini kit (Qiagen, Valencia, CA). RNA was reverse-transcribed using Moloney murine leukemia virus reverse transcriptase (Promega, Madison, WI) and random primers (TOYOBO, Osaka, Japan) after treatment with RQ1DNase I (Promega). Quantitative real-time polymerase chain reaction was performed on a Light Cycler 2.0 (Roche) with the TaqMan Universal PCR Master Mix (Applied Biosystems, Carlsbad, CA). Amplification conditions were 95°C for 10 minutes, then 45 cycles of 95°C for 10 seconds, and 60°C for 30 seconds. All data were normalized to the expression of the glyceraldehyde 3-phosphate dehydrogenase gene. The primer sets and probes are shown in Supplementary Table 1.

### *Cytokine Assay*

LPCs were cultured with 1 μg/mL FSL-1 (Invivogen), 1 μg/mL LPS (Sigma, St Louis, MO), or 1 μg/mL flagellin (Invivogen) for 72 hours at 37°C. The culture supernatants were collected and enzyme-linked immunosorbent assay was performed with the Human Th1/Th2 11plex FlowCytomix kit (eBioscience, San Diego, CA).

### *In Vitro T-Cell Differentiation*

Allogeneic naive $CD4^+$ T cells were co-cultured at 37°C with the indicated cells at a ratio of 1:5 in the presence of 10 U/mL IL-2 (Roche), 2 μg/mL anti-CD3 (BD Biosciences), and 5 μg/mL anti-CD28 (BD Biosciences). After 5 days, cells were analyzed by fluorescence-activated cell sorting. In cytokine blocking experiments, cells were cultured in the presence of 2.5 μg/mL anti–transforming growth factor (TGF)–β, 2.5 μg/mL

anti–IL-1$\beta$, 2.5 $\mu$g/mL anti–IL-6, or 0.5 $\mu$g/mL anti–IL-23 (R&D Systems, Minneapolis, MN).

### *Statistical Analysis*

Differences between the control and experimental groups were evaluated using the Student's $t$ test. Statistical analyses were performed using JMP version 9.02 (SAS Institute, Cary, NC). $P$ values $< .01$ were considered statistically significant.

## Results

### *Phenotypic Characterization of Human Colonic LPC Subsets*

We used a combination of surface markers to characterize LPC subsets in noninvaded colonic tissue samples from colorectal cancer patients. After LPC isolation from colonic tissues, single-cell suspensions were analyzed for expression of lineage markers (CD3, CD19, CD20, and CD56), HLA-DR, CD14, CD11c, and CD163 (Figure 1*A*). To characterize LPCs that were involved in mediating T-cell differentiation and activation, we focused on HLA-DR$^{high}$ cells. HLA-DR$^{high}$ Lin$^-$ cells comprised 3.7%–5.1% of total LPCs, and were divided into 3 subsets: CD14$^-$ CD11c$^{low}$, CD14$^-$ CD11c$^{high}$, and CD14$^+$ CD11c$^+$ cells. CD14$^-$ CD11c$^{low}$ and CD14$^-$ CD11c$^{high}$ cells each did not express CD163 (data not shown), and CD14$^+$ CD11c$^+$ cells were further subdivided into 2 populations: CD163$^{low}$ CD14$^+$ CD11c$^+$ and CD163$^{high}$ CD14$^+$ CD11c$^+$ cells; hereafter, these cells are designated CD14$^+$ CD163$^{low}$ and CD14$^+$ CD163$^{high}$ cells, respectively. In total, human colonic HLA-DR$^{high}$ Lin$^-$ cells comprised 4 subsets: CD14$^+$ CD163$^{low}$ (24.7% $\pm$ 8.2% of all HLA-DR$^{high}$ Lin$^-$ cells), CD14$^+$ CD163$^{high}$ (14.7% $\pm$ 4.7%), CD14$^-$ CD11c$^{high}$ (18.8% $\pm$ 7.9%), and CD14$^-$ CD11c$^{low}$ (30.3% $\pm$ 8.9%) cells (Figure 1*B*). CD14$^+$ CD163$^{low}$ and CD14$^+$ CD163$^{high}$ cells showed macrophage-like morphologies with numerous cytoplasmic vacuoles (Figure 1*C*).

We then analyzed whether these populations were present in other tissues (Figure 1*D*). In the small intestinal

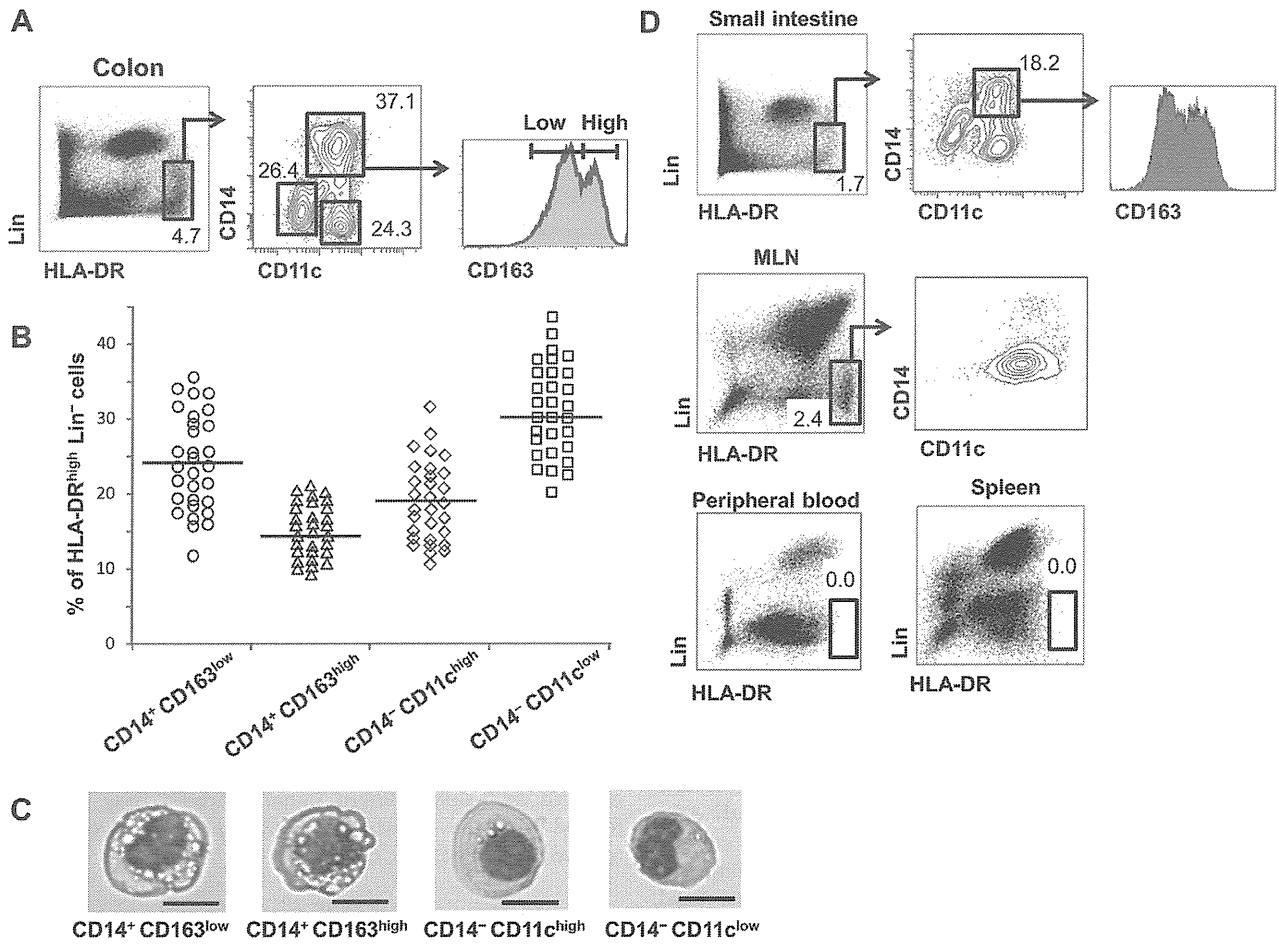


**Figure 1.** Characterization of LPC subsets. (*A*) Flow cytometry analysis of LPCs from normal intestine of colorectal cancer patients. Live HLA-DR$^{high}$ Lin$^-$ cells were gated and analyzed for expression of CD14 vs CD11c (Lin; CD3, CD19, CD20, CD56). Three populations were defined (CD14$^-$ CD11c$^-$, CD14$^-$ CD11c$^+$, and CD14$^+$ CD11c$^+$), and the CD14$^+$ CD11c$^+$ population was further analyzed for CD163 expression. Representative results of 30 independent experiments are shown. (*B*) Percentages of LPC subsets among HLA-DR$^{high}$ Lin$^-$ cells of 30 patients; *horizontal bars* indicate mean. (*C*) Morphological analysis of LPC subsets by May-Grünwald-Giemsa staining. Scale bars = 10 $\mu$m. (*D*) Characterization of cell subsets from human small intestine, MLN, peripheral blood, and spleen. Representative results of 10 independent experiments are shown. *Numbers* indicate the percentage of cells in indicated gates. *Arrows* show gating strategy.

lamina propria, we observed the same 4 populations, albeit with slightly different proportions: $CD14^+$ $CD163^{low}$ (11.7% ± 4.3% of all $HLA\text{-}DR^{high}$ $Lin^-$ cells), $CD14^+$ $CD163^{high}$ (9.9% ± 4.1%), $CD14^-$ $CD11c^{high}$ (35.1% ± 17.2%), and $CD14^-$ $CD11c^{low}$ (33.2% ± 11.1%) cells. In the MLN, we found only small numbers of $CD14^+$ cells and increased numbers of $CD14^-$ $CD11c^{high}$ cells. $HLA\text{-}DR^{high}$ $Lin^-$ cells were not present in peripheral blood and spleen.

Next, we analyzed the surface expressions of several markers on these 4 subsets of human intestinal LPCs (Figure 2). $CD14^+$ $CD163^{low}$ and $CD14^+$ $CD163^{high}$ cells expressed several macrophage and DC markers, including molecules expressed on macrophages (CD16 and CD64), on DCs (CD1c, CD141, CD209, and 6-sulfo LacNAc [slan]), on both macrophages and DCs (CD11b, CD172a, and CD206), and on mature DCs (CD80, CD83, and CD86). These 2 cell subpopulations showed almost the same expression patterns for all examined surface molecules, indicating that CD163 is a unique marker that can distinguish $CD14^+$ cells subpopulations. $CD14^-$ $CD11c^{high}$ cells exhibited high expression of CD1c and CD172a as well as moderate expression of DC maturation markers, but were still heterogeneous because these cells included $CD103^+$ and $CD103^-$ populations. $CD14^-$ $CD11c^{low}$ cells were also heterogeneous, including $CD141^{high}$ and $CD141^-$ populations.

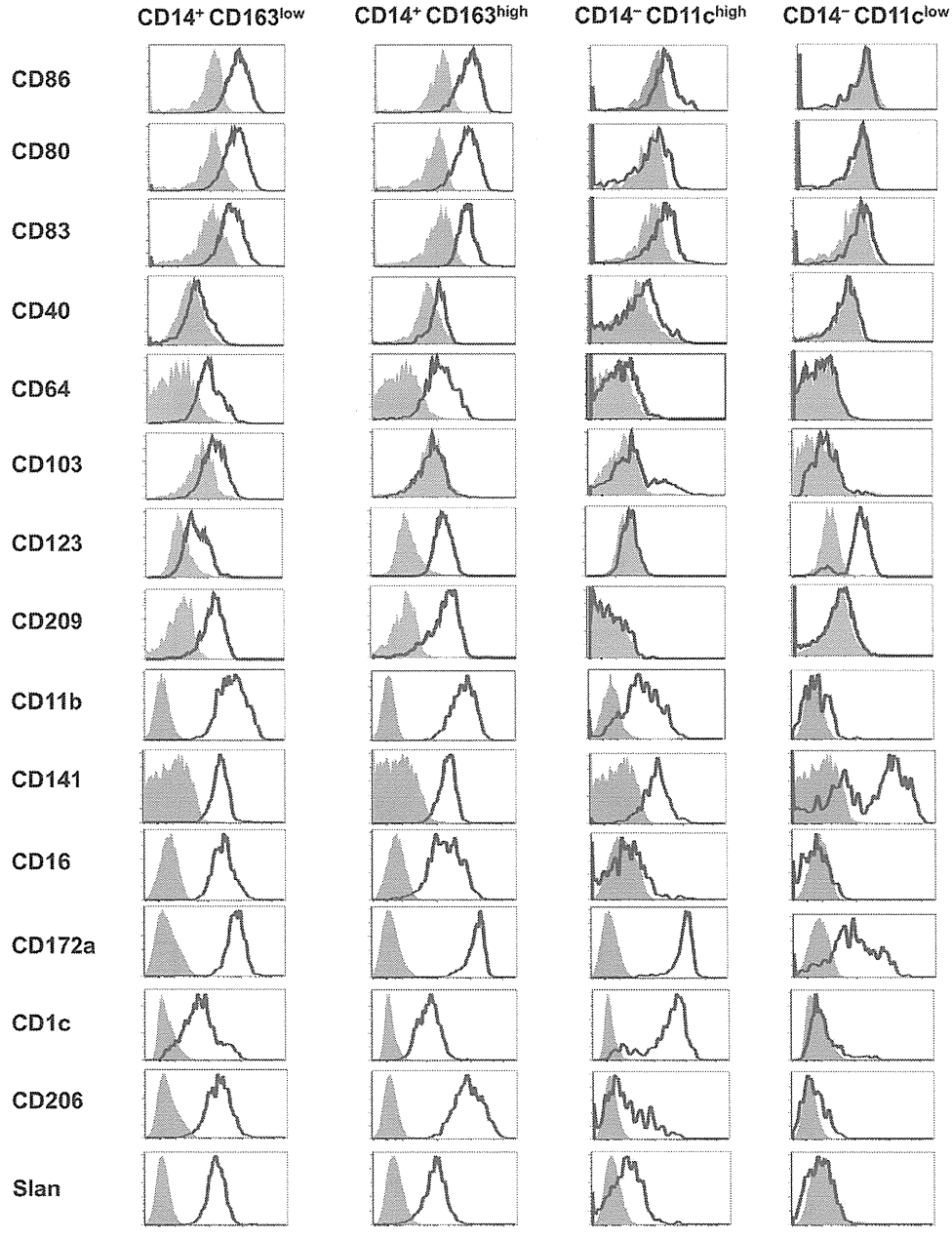


**Figure 2.** Phenotypic analysis of LPC subsets. Flow cytometry for surface expressions of CD86, CD80, CD83, CD40, CD64, CD103, CD123, CD209, CD11b, CD141, CD16, CD172a, CD1c, CD206, and slan in LPC subsets. The histogram shows the profiles of the indicated antibody staining, and the *shaded* histogram shows staining with isotype control. Representative results of 5–11 independent experiments are shown.

### *Gene Expression Features of LPC Subsets*

We performed microarray analysis to compare gene expression profiles among these subsets purified from normal colon of 10 colon cancer patients. To assess the reliability of the microarray analysis, we compared expression of mRNAs encoding glyceraldehyde 3-phosphate dehydrogenase, CD163, CD14, and CD11c across LPC subsets analyzed (Supplementary Figure 1). We found that mRNA expression of these genes correlated with the surface phenotype of each subset. Hierarchical clustering of about 15,000 protein-coding genes with >2-fold change in expression in at least 1 of the 6 pairwise comparisons showed that $CD14^+$ $CD163^{low}$ cells were more closely related to $CD14^+$ $CD163^{high}$ cells than to other subsets (Figure 3*A*). When we selected genes corresponding to the DC-related and monocyte/macrophage-related biological processes (antigen processing and presentation [GO 0019882], phagocytosis [GO 0006909], monocyte differentiation [GO 0030224], or macrophage differentiation [GO 0030225]), the transcriptomic pathways of $CD14^+$ $CD163^{low}$ cells were found to be similar to those of $CD14^+$ $CD163^{high}$ cells. However, when focusing on inflammatory response to antigenic stimulus (GO 0002437), $CD14^+$ $CD163^{low}$ cells were close to $CD14^-$ $CD11c^{high}$ cells (Figure 3*B* and Supplementary Table 2). To gain more insight into the nature of LPC subsets, we analyzed expression of transcription factors and growth factor receptor, which are involved in function and development of DCs and macrophages (Supplementary Figure 2). Expression of mRNAs encoding *MAFB* and *CSFR1* (involved in macrophage differentiation) was high in $CD14^+$ $CD163^{low}$ and $CD14^+$ $CD163^{high}$ cells. $CD14^-$ $CD11c^{high}$ cells expressed the highest level of mRNAs encoding *IRF4* and *FLT3*, which are both involved in the

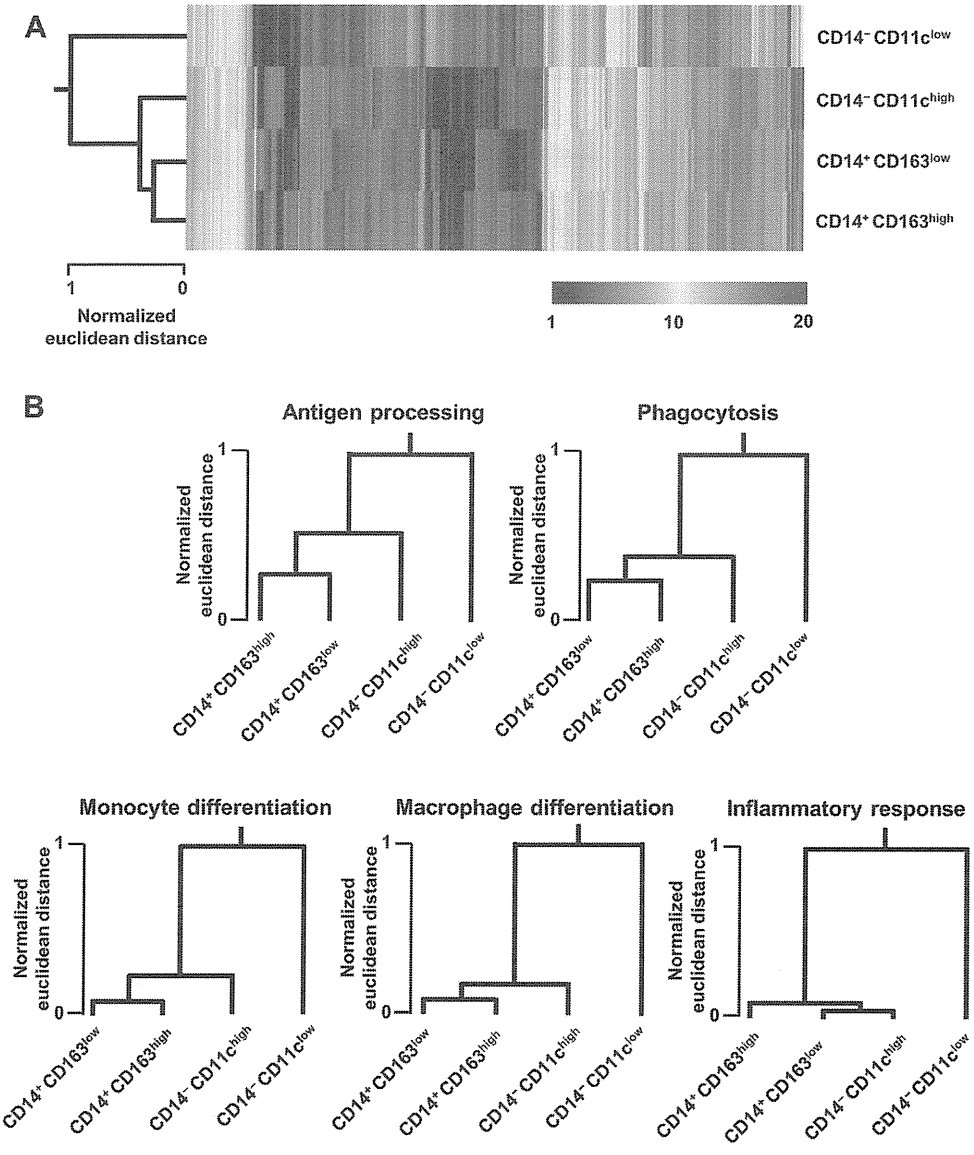


**Figure 3.** Gene expression profiles of LPC subsets. (*A*) Hierarchical clustering and heat map of LPC subsets was generated from about 15,000 protein-coding genes called detected in at least a subset, with >2-fold change in expression in at least 1 of the 6 possible pairwise comparisons. Euclidian distances are divided by the maximum to scale from 0 to 1. (*B*) Hierarchical clustering using sets of differentially expressed genes corresponding to the Gene Ontology biological functions of antigen processing and presentation (203 genes), phagocytosis (66 genes), monocyte differentiation (16 genes), macrophage differentiation (13 genes), or inflammatory response to antigenic stimulus (15 genes). Clustered heat maps were produced by using Euclidean distance. Euclidian distances are divided by the maximum to scale from 0 to 1.

DC differentiation process. $CD14^+$ $CD163^{low}$ cells showed higher levels of *IRF4* and *FLT3* expression than $CD14^+$ $CD163^{high}$ cells. Taken together, these results suggest that $CD14^+$ $CD163^{low}$ cells are closely related to $CD14^+$ $CD163^{high}$ cells and that the developmental pathway of $CD14^+$ $CD163^{low}$ cells have characteristics of both DC and macrophage development.

We next determined the *TLR* mRNA expression of these 4 subsets by quantitative real-time reverse transcription polymerase chain reaction (Figure 4*A*). $CD14^+$ $CD163^{low}$ cells expressed *TLR2* and *TLR4*, $CD14^+$ $CD163^{low}$, and $CD14^+$ $CD163^{high}$ cells expressed *TLR5*, and $CD14^-$ $CD11c^{high}$ cells expressed *TLR9*. $CD14^-$ $CD11c^{low}$ cells did not express any *TLR*. We also examined the gene expressions of several inflammatory and anti-inflammatory mediators (Figure 4*B*). $CD14^+$ $CD163^{low}$ cells exhibited the highest expressions of *IL-6* and *IL-23p19*. $CD14^+$ $CD163^{high}$ cells uniquely expressed several anti-inflammatory markers, including *IL-10, HMOX1,* and *TGFB*. $CD14^-$ $CD11c^{high}$ cells expressed the highest level of *IFNG* among the 4 subsets. *IL-12p35* expression was observed only in $CD14^-$ $CD11c^{low}$ cells. Overall, the 4 subsets of intestinal LPCs showed differential expression patterns of inflammatory genes, and the $CD14^+$

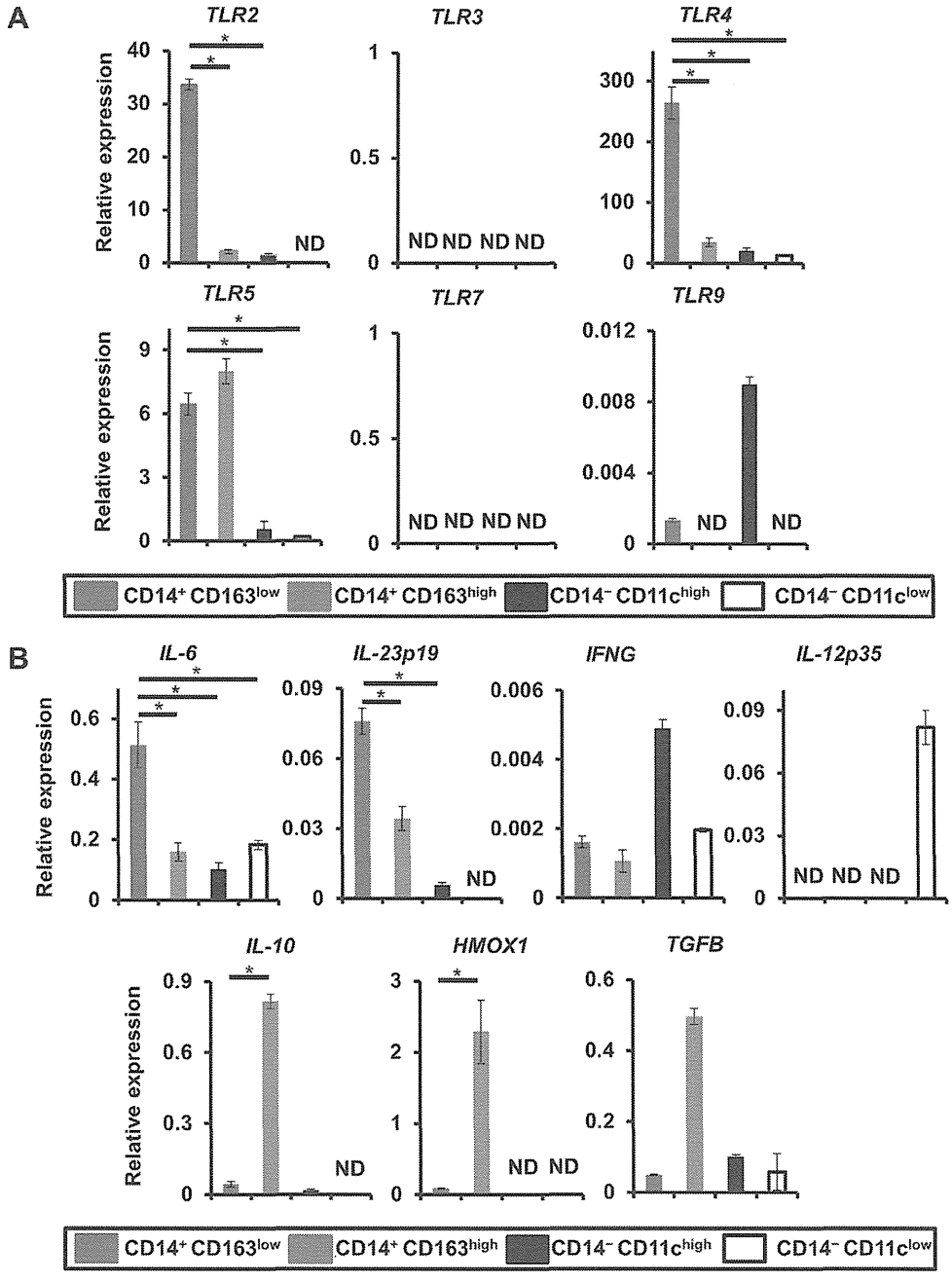


**Figure 4.** Various mRNA expression of LPC subsets. (*A*) Expression of *TLR2, TLR3, TLR4, TLR5, TLR7,* and *TLR9* in LPC subsets. (*B*) Expression of *IL-6, IL-23p19, IFNG, IL-12p35, IL-10, HMOX1,* and *TGFB* in LPC subsets. Results are mean ± SD from 5 independent experiments. ND, not detected. *$P < .01$.

$CD163^{high}$ cells were unique in their expression of anti-inflammatory genes.

### *Cytokine Production of LPC Subsets in Response to TLR Stimulation*

To analyze the functions of these 4 subsets, we used enzyme-linked immunosorbent assay to assess their cytokine productions in response to TLR stimulation (Figure 5). Based on the *TLR* mRNA expression patterns, we used the TLR2 ligand FSL-1, the TLR4 ligand LPS, and the TLR5 ligand flagellin. High production of inflammatory cytokines, such as IL-6, IL-1$\beta$, and TNF-$\alpha$, was observed in the $CD14^+$ $CD163^{low}$ cells, even without stimulation. $CD14^+$ $CD163^{low}$ cells produced increased amounts of IL-6, IL-1$\beta$, and TNF-$\alpha$ in response to LPS, but not in response to FSL-1 or flagellin. $CD14^+$ $CD163^{high}$ cells showed constitutive high production of IL-10, and $CD14^-$ $CD11c^{low}$ cells produced IL-12p70 in response to LPS and flagellin. These findings revealed differential patterns of cytokine production in the 4 LPC subsets, with the $CD14^+$ $CD163^{low}$ cells exhibiting LPS-induced inflammatory responses.

### *Induction of Th17 Cells by $CD14^+$ $CD163^{low}$ Cells*

We next used the allogeneic mixed lymphocyte reaction technique to examine whether the 4 subsets induced Th1 or Th17 cell differentiation. After 5 days of co-culture, the IFN gamma and IL-17 productions of $CD4^+$ T cells were analyzed by intracellular cytokine staining (Figure 6*A*). We used monocyte-derived DCs as a control, which induced IFN-gamma–producing $CD4^+$ T cells (Th1 cells: 15.22% ± 7.19%), but not IL-17–producing $CD4^+$ T cells (Th17 cells: 0%). Naïve $CD4^+$ T cells co-cultured with $CD14^+$ $CD163^{low}$ cells produced high amounts of IL-17 (0.52% ± 0.17%) compared with those co-cultured with other subsets (Figure 6*B*), indicating that $CD14^+$ $CD163^{low}$ cells possess a high capacity

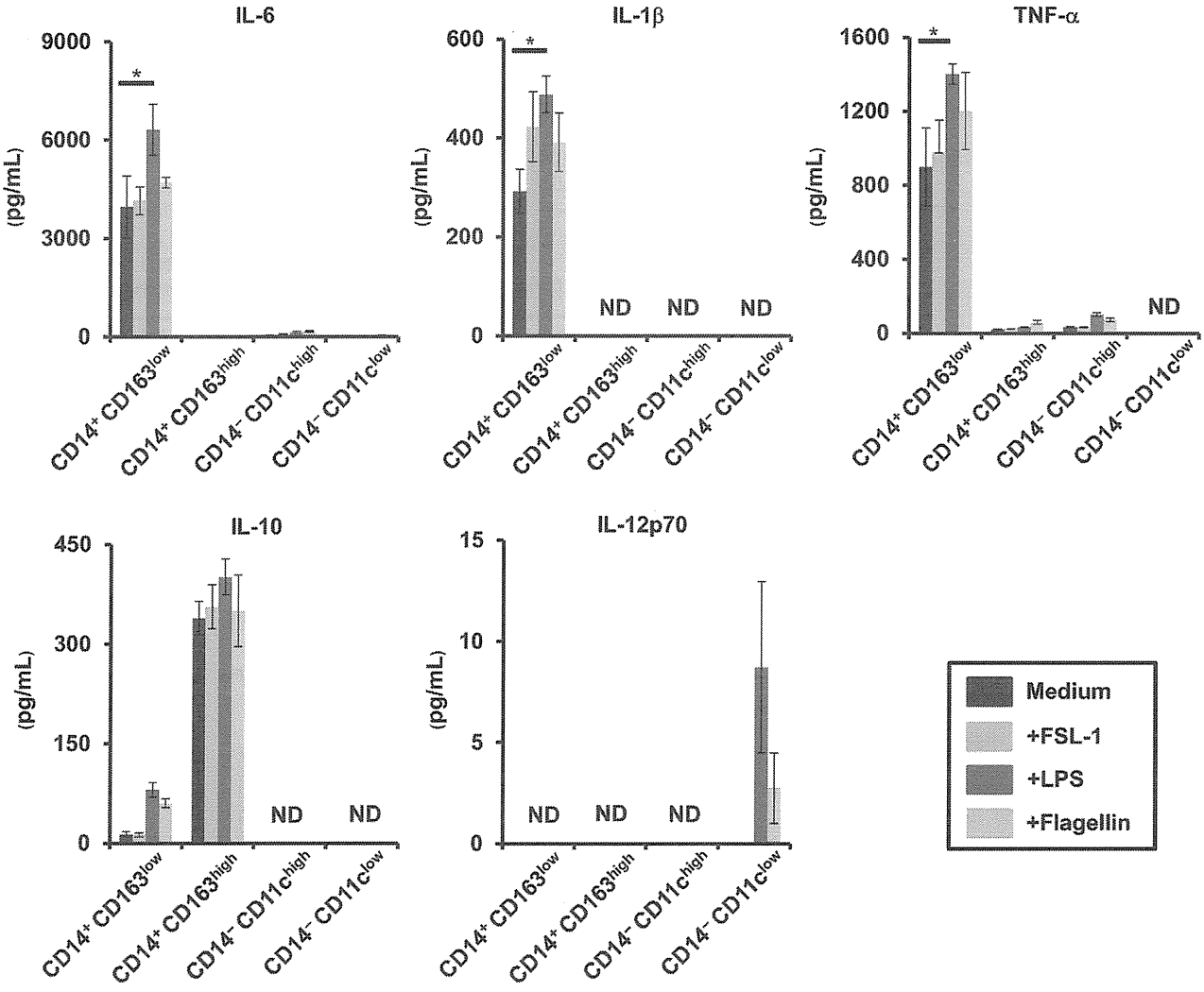


**Figure 5.** Cytokine production of LPC subsets. LPC subsets were analyzed for productions of IL-6, IL-1$\beta$ TNF-$\alpha$, IL-10, and IL-12p70 in response to FSL-1, LPS, or flagellin by enzyme-linked immunosorbent assay. Results are mean ± SD from 5 independent experiments. ND, not detected. *$P < .01$.

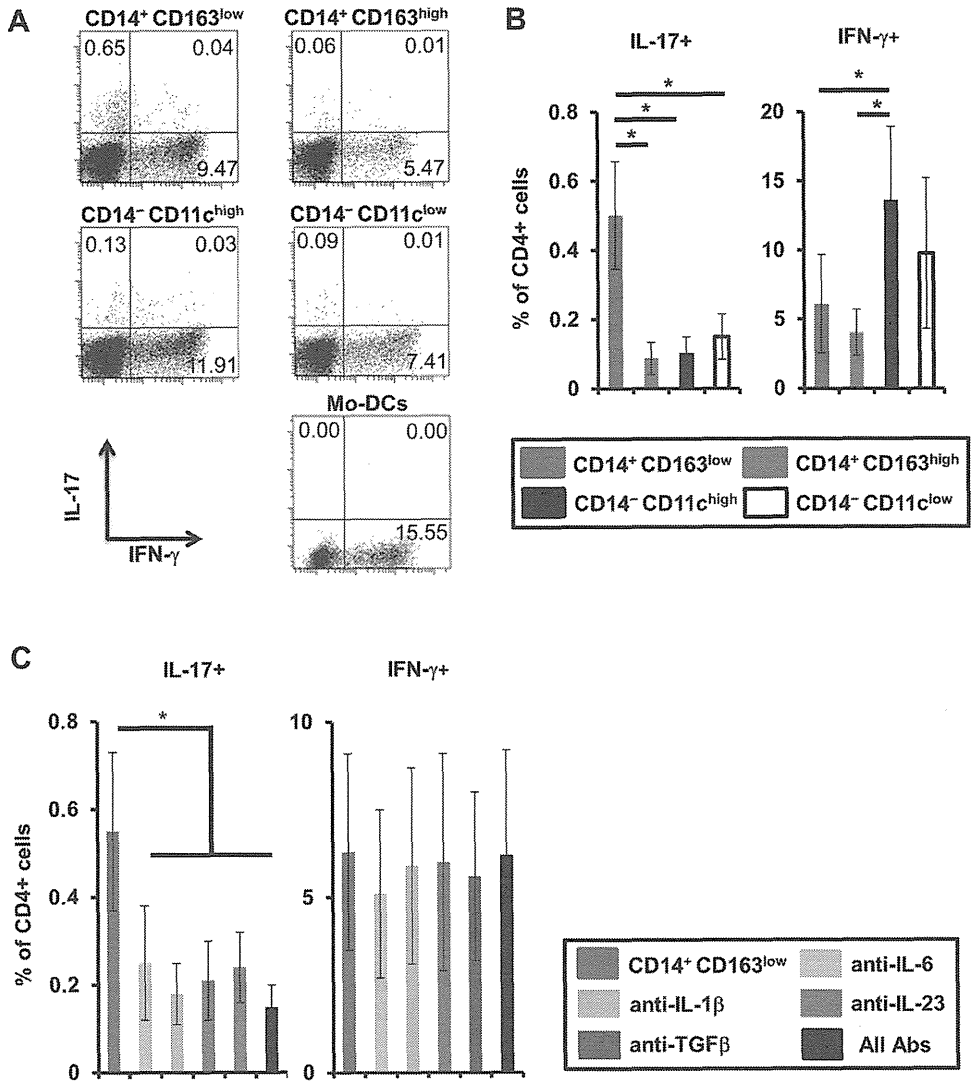


**Figure 6.** Functional properties of T-cell differentiation in LPC subsets. (*A*) Intracellular cytokine staining and flow cytometry performed to evaluate IFN gamma and IL-17 expression by naive T cells after 5 days of co-culture with allogeneic LPC subsets. Co-culture with monocyte-derived DCs was used as a control. Representative results of 8–14 independent experiments are shown. (*B*) Percentages of IL-17–producing cells and IFN gamma–producing cells among the $CD4^+$ cells after co-culture are shown. Results are mean ± SD from 7 independent experiments. $^*P < .01$. (*C*) Intracellular cytokine (IL-17 and IFN gamma) staining of naive T cells after co-culture with allogeneic $CD14^+$ $CD163^{low}$ subsets in the presence or absence of the indicated blocking antibodies. Percentages of IL-17–producing cells and IFN gamma–producing cells among the $CD4^+$ cells are shown. Results are mean ± SD from 5 independent experiments. $^*P < .01$.

to induce Th17 cells. Naïve $CD4^+$ T cells co-cultured with $CD14^-$ $CD11c^{high}$ cells produced high amounts of IFN gamma (13.78% ± 7.02%), indicating that $CD14^-$ $CD11c^{high}$ cells are DCs with a strong ability to induce Th1 cells. $CD14^-$ $CD11c^{low}$ cells induced moderate levels of Th1 cells (9.81% ± 6.75%) and very few, if any, Th17 cells (0.15% ± 0.06%). The $CD14^+$ $CD163^{high}$ cells showed the lowest ability to induce both Th1 and Th17 cells (4.07% ± 1.61% and 0.08% ± 0.04%, respectively). Overall, the 4 LPC subsets had differential activities for inducing Th1 and Th17 cells, with the $CD14^+$ $CD163^{low}$ cells highly inducing Th17 cells.

To analyze the impacts of IL-6, IL-1$\beta$, IL-23, and TGF-$\beta$ on $CD14^+$ $CD163^{low}$ cell-dependent induction of Th17 cells, we blocked the effect of these cytokines using neutralizing antibodies. Th17 cell differentiation by $CD14^+$ $CD163^{low}$ cells was severely impaired in the presence of the blocking antibodies, and Th1 cell differentiation was not affected (Figure 6*C*).

### *Functional Analysis of $CD14^+$ $CD163^{low}$ Cells in CD*

Because $CD14^+$ $CD163^{low}$ cells facilitated Th17 cell differentiation, we next analyzed these cells in CD patients. Among HLA-$DR^{high}$ $Lin^-$ cells, $CD14^+$ $CD163^{low}$ cells were observed almost equally in the noninflamed region of CD (CDn; 28.1% ± 7.1%) and the inflamed region of CD (CDi; 27.2% ± 7.8%) compared with normal colon from colon cancer patients (NC; 25.5 ± 9.4%) (Figure 7*A* and *B*). We also compared the cytokine gene expression of $CD14^+$ $CD163^{low}$ cells between NC, CDn, and CDi. $CD14^+$ $CD163^{low}$ cells in CDi expressed the highest levels of proinflammatory genes, such as *IL-6*, *IL-23p19*, *TNF*, and *IL-12p35*, as well as anti-inflammatory genes, such as *IL-10* and *TGFB*. $CD14^+$ $CD163^{low}$ cells in CDn also expressed higher *IL-6*, *IL-23p19*, and *TNF* and lower *IL-10* compared with those in NC. *TGFB* expression did not differ between $CD14^+$ $CD163^{low}$ cells in NC and CDn (Figure 7*C*). We next compared the abilities of

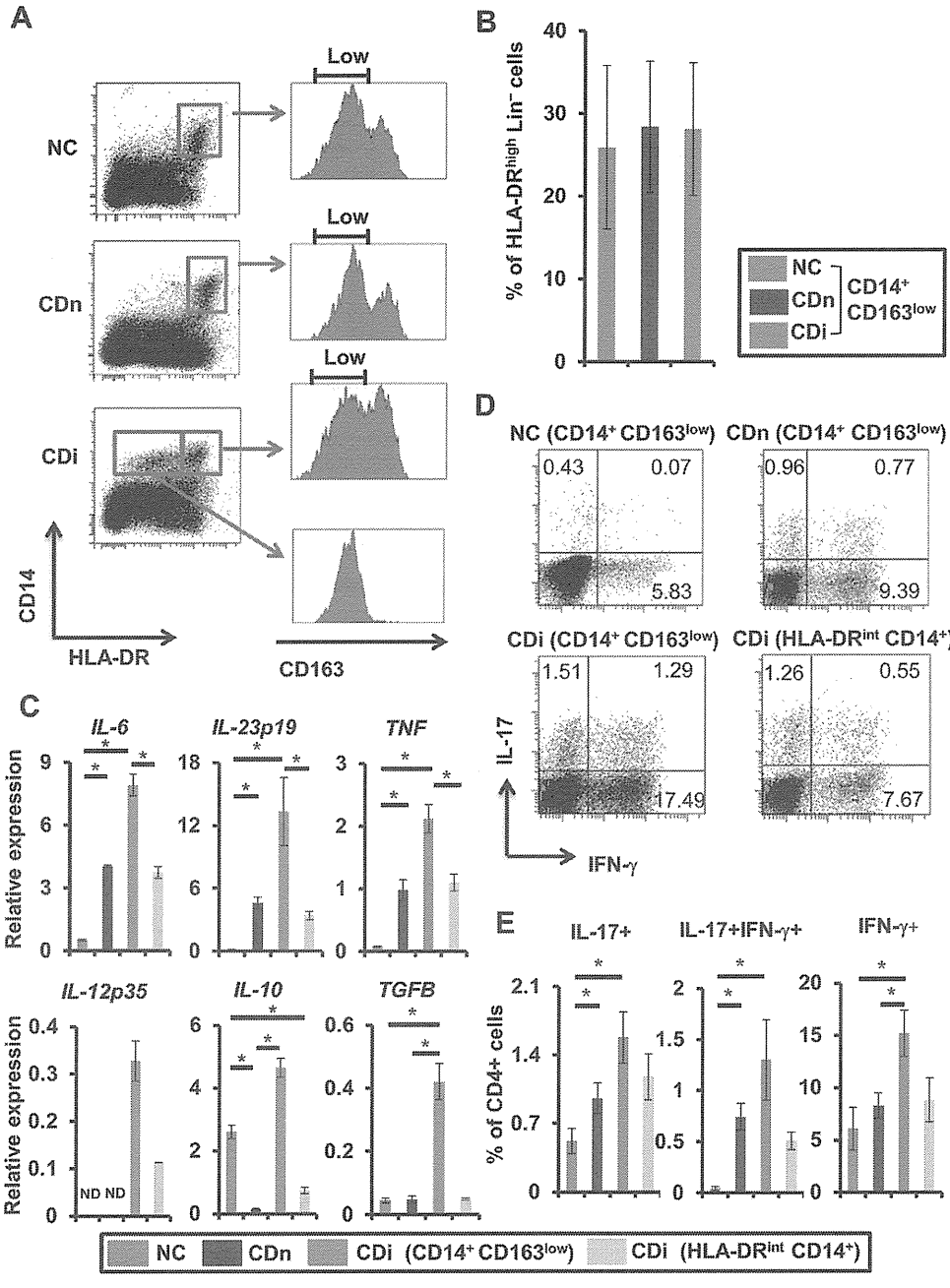


**Figure 7.** $CD14^+$ $CD163^{low}$ cells in Crohn's disease. (*A*) HLA-$DR^{high}$ $CD14^+$ cells were gated and analyzed for CD163 expression in $Lin^-$ cells from NC (n = 30), CDn (n = 22), or CDi (n = 19). Representative results are shown. (*B*) Percentages of $CD14^+$ $CD163^{low}$ cells from NC, CDn, and CDi in HLA-$DR^{high}$ $Lin^-$ cells are shown. (*C*) Expressions of various cytokine mRNAs in $CD14^+$ $CD163^{low}$ cells from NC, CDn, and CDi, and in HLA-$DR^{int}$ $CD14^+$ cells from CDi. Results are mean ± SD from 5 independent experiments. ND, not detected. *$P < .01$. (*D*) Intracellular cytokine (IL-17 and IFN gamma) staining of naive T cells after co-culture with $CD14^+$ $CD163^{low}$ cells from NC, CDn, and CDi, and with HLA-$DR^{int}$ $CD14^+$ cells from CDi. Representative results of 5 independent experiments are shown. (*E*) Percentages of IL-17–producing cells, IL-17/IFN gamma double-producing cells, and IFN gamma–producing cells in $CD4^+$ cells after co-culture. Results are mean ± SD from 5 independent experiments. *$P < .01$.

$CD14^+$ $CD163^{low}$ cells to induce Th1 and Th17 cell differentiation in NC, CDn, and CDi. As mentioned, $CD14^+$ $CD163^{low}$ cells in NC induced approximately 0.5% Th17 cells and few IFN gamma/IL-17 double-producing $CD4^+$ T cells (Th1/17 cells: 0.03% ± 0.01%) (Figure 7*D*). Compared with those in NC, $CD14^+$ $CD163^{low}$ cells in CDn induced similar numbers of Th1 cells (8.31% ± 1.18%), but larger numbers of Th17 (0.96% ± 0.16%) and Th1/17 cells (0.74% ± 0.13%). $CD14^+$ $CD163^{low}$ cells in CDi induced the largest numbers of Th17 cells (1.59% ± 0.26%), Th1/17 cells (1.3% ± 0.39%), and Th1 cells (15.23% ± 2.21%) (Figure 7*D* and *E*).

Interestingly, we found a unique population of HLA-DR intermediate (int) $CD14^+$ cells in CDi. This subset had expression patterns of surface molecules examined similar to $CD14^+$ $CD163^{low}$ cells (Supplementary Figure 3) and high expressions of *IL-6*, *IL-23p19*, and *TNF*, although these levels were lower than those of $CD14^+$ $CD163^{low}$ cells in CDi; these cells also exhibited low *IL-10* expression compared with those in NC (Figure 7*C*). HLA-$DR^{int}$ $CD14^+$ cells induced high levels of Th17 cells (1.18% ± 0.24%) and Th1/17 cells (0.51% ± 0.09%), and moderate levels of Th1 cells (8.83% ± 2.1%) (Figure 7*D* and *E*).

Overall, we found that CD14$^+$ CD163$^{low}$ cells in CDn exhibited high inflammatory cytokine production and strongly induced Th17 cells, and that this ability was further enhanced in CD14$^+$ CD163$^{low}$ cells in CDi. In addition, a unique subset of HLA-DR$^{int}$ CD14$^+$ cells in CDi showed strong ability to produce inflammatory cytokines and to induce Th17 cells.

## Discussion

In this study, we characterized differential functions of 4 LPC subsets in the human colon. Within the HLA-DR$^{high}$ Lin$^-$ population, CD14$^+$ CD163$^{low}$ cells mediated Th17 cell differentiation. In CD patients, this subset had strong capacities for cytokine production and Th17 cell induction. It was recently reported that the CD14$^{high}$ population in human ileal mucosa includes HLA-DR$^{low}$ CD209$^{low}$ CD163$^{low}$, HLA-DR$^{high}$ CD209$^{low}$ CD163$^{low}$, and HLA-DR$^{high}$ CD209$^{high}$ CD163$^{high}$ cells.[28] In terms of the surface molecule expression patterns in these subsets, HLA-DR$^{high}$ CD209$^{low}$ CD163$^{low}$ cells and HLA-DR$^{high}$ CD209$^{high}$ CD163$^{high}$ cells in that report correspond approximately to the CD14$^+$ CD163$^{low}$ cells and CD14$^+$ CD163$^{high}$ cells, respectively, in the present study.

In mice, subsets of intestinal myeloid cells are already well characterized and are distinguished using combinations of surface markers, such as CD11b, CD11c, CD103, or CX3CR1.[16,21,24,29,35] In contrast, the appropriate surface markers for distinguishing myeloid cell subsets in humans remain unknown. In particular, CX3CR1 expression was hardly detected in human intestinal LPCs (unpublished results). In the present study, we found that LPCs in the HLA-DR$^{high}$ Lin$^-$ population could be divided into CD14$^+$ CD163$^{low}$, CD14$^+$ CD163$^{high}$, CD14$^-$ CD11c$^{high}$, and CD14$^-$ CD11c$^{low}$ subsets.

Mouse intestinal subpopulations, such as CX3CR1$^{int}$ and CX3CR1$^{high}$ cells, are present selectively in the intestine, not in MLN and spleen, under steady state.[25,29,36] Mouse CX3CR1$^{int}$ cells, possessing macrophage-like and DC-like activities, highly express CD11c, major histocompatibility complex class II, and the co-stimulatory molecules CD86 and CD80. Consistent with murine CX3CR1$^{int}$ cell expression of both macrophage (F4/80) and DC (DEC205) markers,[29,37,38] here we found that CD14$^+$ CD163$^{low}$ cells expressed both macrophage- and DC-related markers. Gene expression profile analysis also indicates that CD14$^+$ CD163$^{low}$ cells express genes that mediate macrophage- and DC-related functions. In addition, CD14$^+$ CD163$^{low}$ cells exhibited macrophage-like morphology, like the case in intestinal CX3CR1$^+$ cells in mice.[17,28] These findings suggest that human CD14$^+$ CD163$^{low}$ cells might be equivalent to CX3CR1$^{int}$ cells in mice, which are derived from blood monocytes. CD14$^+$ CD163$^{low}$ cells are monocyte-like lineage of cells that gain an ability of DC-related functions after migrating to the intestine. Similarly, a previous study suggests that CD14$^{high}$ macrophages in normal and CD ileum are similar to CX3CR1$^{int}$ cells in mice.[28] We found that CD14$^+$ CD163$^{low}$ cells produced IL-1$\beta$, IL-6, TNF-$\alpha$, and IL-23p19, as well as the anti-inflammatory cytokine IL-10. A recent study in mice suggests that CX3CR1$^{int}$ cells produce not only IL-6 and TNF-$\alpha$, but also low levels of IL-10.[23] In terms of cytokine production patterns, CD14$^+$ CD163$^{low}$ cells in humans are similar to CX3CR1$^{int}$ cells in mice, as found in the phenotypic analyses mentioned previously, further suggesting that CD14$^+$ CD163$^{low}$ cells are a human counterpart to mouse CX3CR1$^{int}$ cells.

There have been several reports analyzing human DC subsets. CD1c$^+$ cells in the intestinal lamina propria express higher levels of activation markers (CD40, CD83, CD86, HLA-DR) than those in blood and produce IL-23 at steady state.[39] The present study indicates that these CD1c$^+$ LPCs are further subdivided into CD14$^+$ CD163$^{low}$, CD14$^+$ CD163$^{high}$ and CD14$^-$ CD11c$^{high}$ cells, and that a main producer of IL-23 is CD14$^+$ CD163$^{low}$ cells. Lung CD1c$^+$ DCs within the CD14$^-$ CD11c$^+$ population activate CD8$^+$ T cells with induction of CD103 expression via TGF-$\beta$.[40] Given the similar expression pattern of surface molecules, the lung CD1c$^+$ CD14$^-$ CD11c$^+$ DCs might correspond to the CD14$^-$ CD11c$^{high}$ subset in the present study. CD141$^{high}$ DCs, a functional homolog of mouse CD103$^+$ DCs, synthesize TNF-$\alpha$, but not IL-12p70, in response to TLR3 stimulation.[41] CD141$^{high}$ cells are present within the CD14$^-$ CD11c$^{low}$ population, which produces IL-12p70 in response to LPS in the present study. In this regard, CD141$^-$ population within the CD14$^-$ CD11c$^{low}$ population might be a IL-12p70 producer. Slan DCs expressing 6-sulfo LacNAc drive Th17/Th1 cell differentiation with production of IL-1$\beta$, IL-23, IL-12, and IL-6 in psoriasis patients.[42] The slan DCs do not express CD14 and CD163. CD14$^+$ CD163$^{low}$ cells expressed 6-sulfo LacNAc, but had no production of IL-12p70. Given the differential profiles of surface marker expression and cytokine production, CD14$^+$ CD163$^{low}$ cells are considered to be a distinct population from slan DCs observed in psoriasis patients.

Th17 cell-associated pro-inflammatory cytokines, such as IL-17 and IL-23, play key roles in several mouse autoimmune disease models and are thought to be involved in the pathogenesis of human immune disorders.[43–47] Several reports have identified innate immune cells driving Th17 differentiation. In mice, CX3CR1$^{int}$ cells in the intestinal LP induce Th17 cells,[24,25] and TLR5$^+$ lamina propria DCs induce Th17 cell differentiation.[35] IRF4–dependent CD11b$^+$ DCs play a key role on Th17 induction.[48,49] Human ovarian tumor cells and tumor-associated antigen-presenting cells reportedly mediate Th17 cell generation at tumor sites.[50] Additionally, a human Th17-inducing inflammatory DC subset derived from blood monocytes was recently identified in synovial fluid of rheumatoid arthritis patients and inflammatory tumor ascites.[51] Human DCs inducing Th17 cell differentiation in the inflammatory condition have been identified; however, it remains unclear which human intestinal

LPC subsets are responsible for Th17 induction at steady state. In the present study, we showed that $CD14^+$ $CD163^{low}$ cells secreted IL-6 and IL-1$\beta$ and differentiated naïve T cells into Th17 cells. $CD14^+$ $CD163^{low}$ cells are the main DCs that induce Th17-mediated immunity in the intestine.

Several recent studies have shown that IBD patients exhibit massive infiltration of Th17 cells in inflamed gastrointestinal mucosa, as well as increased serum IL-17 levels.[52,53] Polymorphisms in the gene encoding the IL-23 receptor are associated with CD.[8] In CD patients, TREM-$1^+$ macrophages are reportedly increased in intestinal mucosa and contribute to intestinal inflammation.[54] Spontaneous production of IL-1$\beta$ and TNF-$\alpha$ is observed in $CD172a^+$ HLA-$DR^+$ cells, which accumulate into MLN and the intestinal mucosa of CD patients.[55] In the present study, we showed that the proportion of $CD14^+$ $CD163^{low}$ cells was not altered between NC and CDn. However, Th17 cell differentiation by $CD14^+$ $CD163^{low}$ cells was significantly higher in CDn than in NC. Abnormal activity of $CD14^+$ $CD163^{low}$ cells is evident, even in the non-inflamed intestine of CD patients. In addition, the $CD14^+$ $CD163^{low}$ cells in CDi had extremely enhanced ability to induce Th17 cells. These results indicated that $CD14^+$ $CD163^{low}$ cells might be involved in the progression of CD via Th17 immunity. Compared with NC and CDn, CDi involved huge numbers of HLA-$DR^{int}$ $CD14^+$ cells. In this regard, HLA-$DR^{int}$ $CD14^+$ cells might migrate from the bloodstream to the intestine in inflammatory environments, as has been reported for mouse $Ly6c^{high}$ $CX3CR1^{int}$ monocytes, which migrate into the intestine during intestinal inflammation.[28]

In conclusion, here we have identified $CD14^+$ $CD163^{low}$ cells as a subset that produces IL-6 and IL-1$\beta$, and can induce Th17 cells in human intestinal lamina propria. Further characterization of human $CD14^+$ $CD163^{low}$ cells showed them to be the putative equivalents of mouse $CX3CR1^{int}$ cells. Based on *TLR* expression and Th17 immunity, $CD14^+$ $CD163^{low}$ cells might play key roles in CD. Our findings suggest that $CD14^+$ $CD163^{low}$ cells could be a new diagnostic and therapeutic target for CD patients.

BASIC AND TRANSLATIONAL AT

## Supplementary Material

Note: To access the supplementary material accompanying this article, visit the online version of *Gastroenterology* at www.gastrojournal.org, and at http://dx.doi.org/10.1053/j.gastro.2013.08.049.

### References


1. Coombes JL, Powrie F. Dendritic cells in intestinal immune regulation. Nat Rev Immunol 2008;8:435–446.
2. Steinman RM, Hawiger D, Nussenzweig MC. Tolerogenic dendritic cells. Annu Rev Immunol 2003;21:685–711.
3. Strober W, Fuss I, Mannon P. The fundamental basis of inflammatory bowel disease. J Clin Invest 2007;117:514–521.
4. Xavier RJ, Podolsky DK. Unravelling the pathogenesis of inflammatory bowel disease. Nature 2007;448:427–434.
5. Neurath MF. IL-23: a master regulator in Crohn disease. Nat Med 2007;13:26–28.
6. Yen D, Cheung J, Scheerens H, et al. IL-23 is essential for T cell-mediated colitis and promotes inflammation via IL-17 and IL-6. J Clin Invest 2006;116:1310–1316.
7. Kobayashi T, Okamoto S, Hisamatsu T, et al. IL23 differentially regulates the Th1/Th17 balance in ulcerative colitis and Crohn's disease. Gut Microbes 2008;57:1682–1689.
8. Duerr RH, Taylor KD, Brant SR, et al. A genome-wide association study identifies IL23R as an inflammatory bowel disease gene. Science 2006;314:1461–1463.
9. Ogura Y, Bonen DK, Inohara N, et al. A frameshift mutation in NOD2 associated with susceptibility to Crohn's disease. Nature 2001; 411:603–606.
10. Hugot JP, Chamaillard M, Zouali H, et al. Association of NOD2 leucine-rich repeat variants with susceptibility to Crohn's disease. Nature 2001;411:599–603.
11. Khor B, Gardet A, Xavier RJ. Genetics and pathogenesis of inflammatory bowel disease. Nature 2011;474:307–317.
12. Barrett JC, Hansoul S, Nicolae DL, et al. Genome-wide association defines more than 30 distinct susceptibility loci for Crohn's disease. Nat Genet 2008;40:955–962.
13. Fisher SA, Tremelling M, Anderson CA, et al. Genetic determinants of ulcerative colitis include the ECM1 locus and five loci implicated in Crohn's disease. Nat Genet 2008;40:710–712.
14. Kayama H, Takeda K. Regulation of intestinal homeostasis by innate and adaptive immunity. Int Immunol 2012;24:673–680.
15. Varol C, Vallon-Eberhard A, Elinav E, et al. Intestinal lamina propria dendritic cell subsets have different origin and functions. Immunity 2009;31:502–512.
16. Schulz O, Jaensson E, Persson EK, et al. Intestinal CD103+, but not CX3CR1+, antigen sampling cells migrate in lymph and serve classical dendritic cell functions. J Exp Med 2009;206:3101–3114.
17. Bogunovic M, Ginhoux F, Helft J, et al. Origin of the lamina propria dendritic cell network. Immunity 2009;31:513–525.
18. Farache J, Koren I, Milo I, et al. Luminal bacteria recruit $CD103^+$ dendritic cells into the intestinal epithelium to sample bacterial antigens for presentation. Immunity 2013;21;38:581–595.
19. McDole JR, Wheeler LW, McDonald KG, et al. Goblet cells deliver luminal antigen to CD103+ dendritic cells in the small intestine. Nature 2012;483:345–349.
20. Jaensson E, Uronen-Hansson H, Pabst O, et al. Small intestinal CD103+ dendritic cells display unique functional properties that are conserved between mice and humans. J Exp Med 2008; 205:2139–2149.
21. Sun CM, Hall JA, Blank RB, et al. Small intestine lamina propria dendritic cells promote de novo generation of Foxp3 T reg cells via retinoic acid. J Exp Med 2007;204:1775–1785.
22. Johansson-Lindbom B, Svensson M, Pabst O, et al. Functional specialization of gut CD103+ dendritic cells in the regulation of tissue-selective T cell homing. J Exp Med 2005;202:1063–1073.
23. Weber B, Saurer L, Schenk M, et al. CX3CR1 defines functionally distinct intestinal mononuclear phagocyte subsets which maintain their respective functions during homeostatic and inflammatory conditions. Eur J Immunol 2011;41:773–779.
24. Denning TL, Wang YC, Patel SR, et al. Lamina propria macrophages and dendritic cells differentially induce regulatory and interleukin 17-producing T cell responses. Nat Immunol 2007;8:1086–1094.
25. **Atarashi K, Nishimura J**, Shima T, et al. ATP drives lamina propria TH17 cell differentiation. Nature 2008;455:808–812.
26. Zigmond E, Varol C, Farache J, et al. Ly6C hi monocytes in the inflamed colon give rise to proinflammatory effector cells and migratory antigen-presenting cells. Immunity 2012;37:1076–1090.
27. Rivollier A, He J, Kole A, et al. Inflammation switches the differentiation program of $Ly6C^{hi}$ monocytes from antiinflammatory macrophages to inflammatory dendritic cells in the colon. J Exp Med 2012; 209:139–155.
28. Bain CC, Scott CL, Uronen-Hansson H, et al. Resident and pro-inflammatory macrophages in the colon represent alternative

context-dependent fates of the same Ly6C$^{hi}$ monocyte precursors. Mucosal Immunol 2013;6:498–510.
29. Kayama H, Ueda Y, Sawa Y, et al. Intestinal CX3C chemokine receptor 1 high (CX3CR1$^{high}$) myeloid cells prevent T-cell-dependent colitis. Proc Natl Acad Sci U S A 2012;109:5010–5015.
30. Hadis U, Wahl B, Schulz O, et al. Intestinal tolerance requires gut homing and expansion of FoxP3$^{+}$ regulatory T cells in the lamina propria. Immunity 2011;34:237–246.
31. Smythies LE. Human intestinal macrophages display profound inflammatory anergy despite avid phagocytic and bacteriocidal activity. J Clin Invest 2005;115:66–75.
32. Smith PD, Smythies LE, Mosteller-Barnum M, et al. Intestinal macrophages lack CD14 and CD89 and consequently are down-regulated for LPS- and IgA-mediated activities. J Immunol 2001; 164:2651–2656.
33. Kamada N, Hisamatsu T, Okamoto S, et al. Unique CD14 intestinal macrophages contribute to the pathogenesis of Crohn disease via IL-23/IFN-gamma axis. J Clin Invest 2008;118:2269–2280.
34. Kamada N, Hisamatsu T, Honda H, et al. Human CD14+ macrophages in intestinal lamina propria exhibit potent antigen-presenting ability. J Immunol 2009;183:1724–1731.
35. Uematsu S, Fujimoto K, Jang MH, et al. Regulation of humoral and cellular gut immunity by lamina propria dendritic cells expressing Toll-like receptor 5. Nat Immunol 2008;9:769–776.
36. Diehl GE, Longman RS, Zhang JX, et al. Microbiota restricts trafficking of bacteria to mesenteric lymph nodes by CX3CR1$^{hi}$ cells. Nature 2013;494:116–120.
37. Tamoutounour S, Henri S, Lelouard H, et al. CD64 distinguishes macrophages from dendritic cells in the gut and reveals the Th1-inducing role of mesenteric lymph node macrophages during colitis. Eur J Immunol 2012;42:1–17.
38. Niess JH, Adler G. Enteric flora expands gut lamina propria CX3CR1$^{+}$ dendritic cells supporting inflammatory immune responses under normal and inflammatory conditions. J Immunol 2010; 184:2026–2037.
39. Dillon SM, Rogers LM, Howe R, et al. Human intestinal lamina propria CD1c+ dendritic cells display an activated phenotype at steady state and produce IL-23 in response to TLR7/8 stimulation. J Immunol 2010;184:6612–6621.
40. Yu CI, Becker C, Wang Y, et al. Human CD1c+ dendritic cells drive the differentiation of CD103+ CD8+ mucosal effector T cells via the cytokine TGF-beta. Immunity 2013;38:818–830.
41. Haniffa M, Shin A, Bigley V, et al. Human tissues contain CD141hi cross-presenting dendritic cells with functional homology to mouse CD103+ nonlymphoid dendritic cells. Immunity 2012;37:60–73.
42. Hansel A, Gunther C, Ingwersen J, et al. Human slan (6-sulfo LacNAc) dendritic cells are inflammatory dermal dendritic cells in psoriasis and drive strong TH17/TH1 T-cell responses. J Allergy Clin Immunol 2011;127:787–794.
43. Wong CK, Lit LC, Tam LS, et al. Hyperproduction of IL-23 and IL-17 in patients with systemic lupus erythematosus: implications for Th17-mediated inflammation in auto-immunity. Clin Immunol 2008; 127:385–393.
44. Ma HL, Liang S, Li J, et al. IL-22 is required for Th17 cell–mediated pathology in a mouse model of psoriasis-like skin inflammation. J Clin Invest 2008;118:597–607.
45. Komiyama Y, Nakae S, Matsuki T, et al. IL–17 Plays an important role in the development of experimental autoimmune encephalomyelitis. J Immunol 2006;177:566–573.
46. Chan JR, Blumenschein W, Murphy E, et al. IL-23 stimulates epidermal hyperplasia via TNF and IL-20R2-dependent mechanisms with implications for psoriasis pathogenesis. J Exp Med 2006; 203:2577–2587.
47. Kurosawa K, Hirose K, Sano H, et al. Increased Interleukin-17 production in patients with systemic sclerosis. Arthritis Rheum 2000; 43:2455–2463.
48. Schlitzer A, McGovern N, Teo P, et al. IRF4 Transcription factor-dependent CD11b+ dendritic cells in human and mouse control mucosal IL-17 cytokine responses. Immunity 2013;38:970–983.
49. Persson EK, Uronen-Hansson H, Semmrich M, et al. IRF4 transcription-factor dependent CD103+CD11b+ dendritic cells drive mucosal T helper 17 cell differentiation. Immunity 2013; 38:958–969.
50. Miyahara Y, Odunsi K, Chen W, et al. Generation and regulation of human CD4$^{+}$ IL-17-producing T cells in ovarian cancer. Proc Natl Acad Sci U S A 2008;105:15505–15510.
51. Segura E, Touzot M, Bohineust A, et al. Human inflammatory dendritic cells induce th17 cell differentiation. Immunity 2013;38:336–348.
52. Veny M, Esteller M, Ricart E, et al. Late Crohn's disease patients present an increase in peripheral Th17 cells and cytokine production compared with early patients. Aliment Pharmacol Ther 2010; 31:561–572.
53. Fujino S, Andoh A, Bamba S, et al. Increased expression of interleukin 17 in inflammatory bowel disease. Gut 2003;52:65–70.
54. Schenk M, Bouchon A, Seibold F, et al. TREM-1-expressing intestinal macrophages crucially amplify chronic inflammation in experimental colitis and inflammatory bowel diseases. J Clin Invest 2007; 117:3097–3106.
55. Baba N, Van VQ, Wakahara K, et al. CD47 fusion protein targets CD172a+ cells in Crohn's disease and dampens the production of IL-1$\beta$ and TNF. J Exp Med 2013;210:1251–1263.

**Author names in bold designate shared co-first authorship.**

**Received March 29, 2013. Accepted August 22, 2013.**

*Reprint requests*

**Address requests for reprints to: Junichi Nishimura, MD, PhD, Department of Gastroenterological Surgery, Graduate School of Medicine, Osaka University, Yamadaoka 2-2, Suita City, Osaka 565-0871, Japan. e-mail: jnishimura@gesurg.med.osaka-u.ac.jp; fax: 81(0)6 6879 3259; or Kiyoshi Takeda, MD, PhD, Laboratory of Immune Regulation, Graduate School of Medicine, Osaka University, Yamadaoka 2-2, Suita City, Osaka 565-0871, Japan.**
**e-mail: ktakeda@ongene.med.osaka-u.ac.jp; fax: 81(0)6 6879 3989.**

*Conflicts of interest*

**The authors disclose no conflicts.**

## Supplementary Material

### *Antibodies for Flow Cytometry*

The following antibodies were used: phycoerythrin (PE)-conjugated anti-CD3 (HIT3a; BD Biosciences), anti-CD19 (SJ25C1; BD Biosciences), anti-CD20 (2H7; BD Biosciences), anti-CD56 (B159; BD Biosciences), fluorescein isothiocyanate–conjugated anti-CD14 (MφP9; BD Biosciences), allophycocyanin-conjugated anti-CD11c (B-ly6; BD Biosciences), PE-Cy7–conjugated anti–HLA-DR (L243; Biolegend, San Diego, CA), peridinin chlorophyll protein complex-Cy5.5-conjugated anti-CD163 (GHI61; Biolegend), fluorescein isothiocyanate–conjugated anti-lineage (BD Biosciences), PE-Cy5–conjugated anti-CD86 (2331; BD Biosciences), anti-CD80 (L307.4; BD Biosciences), anti-CD83 (HB15e; BD Biosciences), anti-CD40 (5C3; BD Biosciences), PE-conjugated anti-CD64 (10.1; BD Biosciences), anti-CD103 (Ber-ACT8; Biolegend), anti-CD123 (7G3; BD Biosciences), anti-CD209 (DCN46; BD Biosciences), anti-CD11b (ICRF44; Biolegend), anti-CD141 (M80; Biolegend), anti-CD16 (3G8; BD Biosciences), anti-CD172a (SE5A5; Biolegend), anti-CD206 (15-2; Biolegend), anti-slan (DD-1; Miltenyi Biotec, Bergisch Gladbach, Germany), Brilliant Violet-conjugated anti-CD1c (L161; Biolegend), peridinin chlorophyll protein complex-Cy5.5-conjugated anti-CD4 (SK3; BD Biosciences), PE-conjugated anti-IL17A (N49-653; BD Biosciences), allophycocyanin-conjugated anti–IL-4 (MP4-25D2; BD Biosciences), and fluorescein isothiocyanate–conjugated anti–IFN-gamma (B27; BD Biosciences).

### *Intracellular Cytokine Analysis*

$CD4^+$ T cells were stimulated for 4 hours in the presence of 5 μM calcium ionosphere (Sigma), 50 ng/mL phorbol myristate acetate (Sigma), and GolgiStop (BD Biosciences). Intracellular cytokine staining was subsequently performed with fixation and permeabilization buffers.

### *Preparation of Monocyte-Derived DCs*

Peripheral $CD14^+$ monocytes were isolated from peripheral blood monocytes using CD14 microbeads (Miltenyi Biotec) following the manufacturer's instructions. For in vitro monocyte-derived DC differentiation, $CD14^+$ monocytes were cultured for 5 days in RPMI 1640 containing 10% fetal bovine serum, with 100 ng/mL recombinant human granulocyte macrophage colony-stimulating factor (Primmune, Kobe, Japan) and 100 U/mL recombinant human IL-4 (Primmune).

### *Microarray Analysis*

Gene expression analysis using SurePrint G3 Human Gene Expression v2 8x60K Microarray (G4845A) (Agilent Technologies) was performed as one color experiments by the Dragon Genomics Center (TaKaRa Bio Inc., Shiga, Japan). Total RNA from $CD163^{high}$ ($CD14^+$ $CD163^{high}$), $CD163^{low}$ ($CD14^+$ $CD163^{low}$), DN ($CD14^-$ $CD11c^{low}$) and CD11c ($CD14^-$ $CD11c^{high}$) cells, which were derived from the sorted $HLA\text{-}DR^{high}$ $Lin^-$ LPC subsets in noninvaded colonic tissue samples from individual colorectal cancer patients (n = 10) was extracted using RNeasy kit (Qiagen) following manufacturer's instructions. Twenty nanograms total RNA was reverse transcribed into double strand complementary DNAs by using an Ovation Pico WTA System V2 (NuGen) following manufacturer's protocol. Resulting complementary DNAs were subsequently used for in vitro transcription by DNA polymerase and labeled with cyanine-3 using a Genomic DNA Enzymatic Labeling Kit (Agilent Technologies) according to the manufacturer's protocol. After labeling, the labeled 2 μg of each complementary DNA sample was then hybridized on SurePrint G3 Human Gene Expression v2 8x60K Microarray at 65°C for 17 hours with rotation in the dark. Hybridization was performed using a Gene Expression Hybridization Kit (Agilent Technologies) following the manufacturer's instructions. After washing in GE washing buffer, slides were scanned with an Agilent Microarray Scanner G2505C. Feature extraction software (version 10.10.1.1) was used to convert images into gene expression data. Raw data were imported into GeneSpring GX 11.0 (Agilent Technologies) for database management and quality control. This normalized data without the threshold raw signal and the global normalization algorithm was used for identifying differentially expressed genes. Raw data have been accepted in Gene Expression Omnibus, a public repository for microarray data, aimed at storing Minimum Information About Microarray Experiments Access to data concerning this study is found under Gene Expression Omnibus experiment accession number GSE49066.

Cell Host & Microbe
Article

# A Single Strain of *Clostridium butyricum* Induces Intestinal IL-10-Producing Macrophages to Suppress Acute Experimental Colitis in Mice

Atsushi Hayashi,[1,3] Toshiro Sato,[1] Nobuhiko Kamada,[4] Yohei Mikami,[1,2] Katsuyoshi Matsuoka,[1] Tadakazu Hisamatsu,[1] Toshifumi Hibi,[1] Axel Roers,[5] Hideo Yagita,[6] Toshiaki Ohteki,[7,8] Akihiko Yoshimura,[2,8] and Takanori Kanai[1,*]

[1]Division of Gastroenterology and Hepatology, Department of Internal Medicine
[2]Department of Microbiology and Immunology
Keio University School of Medicine, Tokyo 160-8582, Japan
[3]Research Laboratory, Miyarisan Pharmaceutical, Tokyo 114-0016, Japan
[4]Department of Pathology and Comprehensive Cancer Center, University of Michigan Medical School, Ann Arbor, MI 48109, USA
[5]Institute for Immunology, Medical Faculty Carl Gustav Carus, University of Technology Dresden, 01307 Dresden, Germany
[6]Department of Immunology, Juntendo University School of Medicine, Tokyo 113-8421, Japan
[7]Department of Biodefense Research, Medical Research Institute, Tokyo Medical and Dental University, Tokyo 113-8510, Japan
[8]Core Research for Evolutional Science and Technology, Japan Science and Technology Agency, Tokyo 102-0081, Japan
*Correspondence: takagast@z2.keio.jp
http://dx.doi.org/10.1016/j.chom.2013.05.013

## SUMMARY

Imbalance in gut bacterial composition provokes host proinflammatory responses causing diseases such as colitis. Colonization with a mixture of *Clostridium* species from clusters IV and XIVa was shown to suppress colitis through the induction of IL-10-producing regulatory T (Treg) cells. We demonstrate that a distinct *Clostridium* strain from cluster I, *Clostridium butyricum* (*CB*), prevents acute experimental colitis in mice through induction of IL-10, an anti-inflammatory cytokine. However, while *CB* treatment had no effect on IL-10 production by T cells, IL-10-producing F4/80$^+$CD11b$^+$CD11c$^{int}$ macrophages accumulated in the inflamed mucosa after *CB* treatment. *CB* directly triggered IL-10 production by intestinal macrophages in inflamed mucosa via the TLR2/MyD88 pathway. The colitis-preventing effect of *CB* was negated in macrophage-specific IL-10-deficient mice, suggesting that induction of IL-10 by intestinal macrophages is crucial for the probiotic action of *CB*. Collectively, *CB* promotes IL-10 production by intestinal macrophages in inflamed mucosa, thereby preventing experimental colitis in mice.

## INTRODUCTION

The human gastrointestinal tract harbors approximately $10^{14}$ commensal bacteria of over 1,000 species. The profile of bacterial species can vary between individuals and is determined by a variety of factors (Gill et al., 2006; Honda and Littman, 2012; Ley et al., 2006). Intestinal microbiota contribute to many host physiological processes, including nutrient acquisition and development of the gut-specific immune system, as well as protection from infectious pathogens. The host in turn provides niches and nutrients for the commensal bacteria (Garrett et al., 2010; Hooper et al., 2012). To maintain the mutually beneficial relationship between host and commensal microorganisms, the host immune system shapes the compositional balance of symbiotic commensal bacteria (Hooper et al., 2012). Recent studies have revealed that an imbalance in the bacterial composition (dysbiosis) provokes host proinflammatory immune responses and induces various inflammatory and metabolic diseases (Elinav et al., 2011; Garrett et al., 2007; Vijay-Kumar et al., 2010).

In a conventional environment, the gut bacterial community forms hierarchies in which only a selected group of bacteria occupy the mucosal layer and surface of the epithelium; thus, nonselected bacteria are expelled from the mucosal surface. Competition in the bacterial community plays a pivotal role in the prevention of pathogenic bacteria invasion. However, the sequestration of microbiota confounds the immunological analysis of host versus specific bacteria. Recent advances in gnotobiotic technology have enabled analysis of the role of specific bacterial strains in immunological responses (Chinen and Rudensky, 2012; Geuking et al., 2011; Tlaskalová-Hogenová et al., 2011). Using these techniques, a recent study reported that a complex mixture of 46 strains of *Clostridium* induced TGF-β in intestinal epithelial cells that promoted the subsequent accumulation of interleukin-10 (IL-10)-producing induced T regulatory (iTreg) cells, which suppressed colitis in a dextran sodium sulfate (DSS) colitis model (Atarashi et al., 2011). However, T cells might be dispensable for acute DSS colitis (Katakura et al., 2005), bringing into question the role of iTreg cells in the probiotic effects of *Clostridium* species.

Unlike the mixture of 46 strains of *Clostridium* in *Clostridium* clusters IV and XIVa, *Clostridium butyricum* (*CB*), which is used as a probiotic in clinical practice (Seki et al., 2003) is classified in *Clostridium* cluster I and is a group member of allochthonous bacteria in specific pathogen-free (SPF) conditions (Sato and Tanaka, 1997). In the present study, we demonstrated that administration of the probiotic bacterial strain *CB* prevented experimental colitis via an IL-10-dependent mechanism. *CB*